

1  
2  
3  
4 **1 A depositional model for deep-lacustrine, partially confined,**  
5 **2 turbidite fans: early Cretaceous, North Falkland Basin**

6  
7  
8 3 Thomas J.H. Dodd\*<sup>1</sup>, Dave J. McCarthy<sup>1</sup> and Philip C. Richards  
9  
10 4

11 5 *<sup>1</sup>British Geological Survey, the Lyell Centre, Research Avenue South, Edinburgh,*  
12 *EH14 4AP, United Kingdom, [tdodd@bgs.ac.uk](mailto:tdodd@bgs.ac.uk)*

13  
14 **7 ABSTRACT**  
15

16 8 This paper presents a model of facies distribution within a set of early Cretaceous,  
17 9 deep-lacustrine, partially confined turbidite fans (Sea Lion Fan, Sea Lion North Fan,  
18 10 Otter Fan) in the North Falkland Basin, South Atlantic. As a whole, ancient deep-  
19 11 lacustrine turbidite systems are underrepresented in the literature when compared  
20 12 with those documented in marine basins. Lacustrine turbidite systems can form  
21 13 extensive, good quality hydrocarbon reservoirs, making the understanding of such  
22 14 systems crucial to exploration within lacustrine basins. An integrated analysis of  
23 15 seismic cross sections, seismic amplitude extraction maps, and 455 m of core has  
24 16 enabled the identification of a series of turbidite fans. The deposits of these fans  
25 17 have been separated into lobe axis, lobe fringe and lobe distal fringe settings.  
26 18 Seismic architectures, observed in the seismic amplitude extraction maps, are  
27 19 interpreted to represent geologically associated heterogeneities, including: feeder  
28 20 systems, terminal mouth lobes, flow deflection, sinuous lobe axis deposits, flow  
29 21 constriction and stranded lobe fringe areas. When found in combination, these  
30 22 architectures suggest “partial confinement” of a system, something that appears to  
31 23 be a key feature in the lacustrine turbidite setting of the North Falkland Basin. Partial  
32 24 confinement of a system occurs when positionally generated topography controls  
33 25 the flow-pathway and deposition of subsequent turbidite fan deposits. The term  
34 26 “partial confinement” provides a term for categorising a system whose depositional  
35 27 boundaries are unconfined by the margins of the basin, yet exhibit evidence of  
36 28 internal confinement, primarily controlled by depositional topography. Understanding  
37 29 the controls that dictate partial confinement; and the resultant distribution of sand-  
38 30 prone facies within deep-lacustrine turbidite fans, is important, particularly  
39 31 considering their recent rise as hydrocarbon reservoirs in rift and failed-rift settings.  
40  
41  
42  
43  
44  
45  
46  
47  
48  
49  
50  
51  
52  
53  
54  
55  
56  
57  
58  
59  
60

- 1 **Keywords:** Turbidites, North Falkland Basin, Sea Lion Fan, Partial Confinement,
- 2 Hybrid Event Bed, Deep-Lacustrine.

1  
2  
3  
4  
5  
6  
7  
8  
9  
10  
11  
12  
13  
14  
15  
16  
17  
18  
19  
20  
21  
22  
23  
24  
25  
26  
27  
28  
29  
30  
31  
32  
33  
34  
35  
36  
37  
38  
39  
40  
41  
42  
43  
44  
45  
46  
47  
48  
49  
50  
51  
52  
53  
54  
55  
56  
57  
58  
59  
60

## **INTRODUCTION**

There is a significant body of published research on marine turbidite systems that form a large proportion of the world's major hydrocarbon reservoirs (Fugitt et al., 2000; Hempton et al., 2005; Mayall et al., 2006; Saller et al., 2008; Shanmugam et al., 2009). Despite there being a reasonable amount of published literature on modern-day lakes such as Lake Malawi, Africa (Crossley, 1984; Scholz et al., 1990; Lyons et al., 2011) and Lake Baikal, Russia (Nelson et al., 1999), and a proportion of literature addressing the ancient depositional environment as a whole (Buatois et al., 1996; Larsen and Smith, 1999; Saez and Cabrera, 2002; Moernaut et al., 2014), there is still relatively little in the way of published material describing the facies, facies architecture and development of ancient deep-lacustrine turbidites. Furthermore, there is a scarcity of literature that focuses on comparing and contrasting lacustrine systems and their marine counterparts.

Deep-lacustrine turbidite systems, form important hydrocarbon reservoirs and trapping geometries in a number of basins worldwide, such as: the Suphan Buri Basin, Thailand (Ronghe and Surarat, 2002), the Songliao Basin, China (Zhi-qiang et al., 2010), the Bohai Bay Basin, China (Zhang, 2004; Li et al., 2014) and the pre-salt rift basins of West Africa (Jungslager, 1999; MacDonald et al., 2003). A good example comes from the Lucian Formation, offshore South Gabon, where extreme variations in thickness and reservoir heterogeneity occur as a result of confinement of high-density turbidites along fault-related lake-floor depressions (Smith, 1995). These few examples suggest that lacustrine turbidite fans can be particularly heterogeneous and therefore may offer a different set of challenges to model than compared with marine systems.

### **Level of confinement: partially confined turbidite systems**

Fully confined turbidite systems are restricted by encircling topography and have been referred to as ponded systems (Winker, 1996) or confined or contained systems (Southern et al., 2015) and are discussed further in Smith (1995). Other examples of turbidite systems are affected by confining topography, but are not fully restricted by encircling basin topography (e.g. Lomas and Joseph, 2004). Confining topography can be formed by: lateral or downstream basin margins (Amy et al., 2004; Kane et al., 2010; Southern et al., 2014); structural features on the basin floor

1 (Davis et al., 2009); or depositionally generated topography on the basin floor (i.e.  
2 lobe compensation; Mutti and Normark 1987; Straub and Pyles, 2012).

3 The term “partial-confinement” is used here in the depositional model for the Sea  
4 Lion Fan and refers to a system whose broad depositional boundaries are not  
5 restricted by encircling topography, the down-stream limits are largely unconfined,  
6 but evidence exists for confinement of internal geometries (within the fan).  
7 Confinement of internal geometries is likely generated by depositional topography,  
8 which controlled the distribution of subsequent turbidite flows. High flow efficiencies,  
9 in particular high flow volumes, may have produced more elongate fan deposits (Al  
10 Ja’Aidi et al., 2004) and therefore elongated depositional topography. Ultimately,  
11 partial confinement may result in fan deposits with more laterally constrained facies  
12 belts compared with examples from unconfined systems (Shanmugam and Muiola,  
13 1988; Covault and Romans, 2009). If partial confinement is restricted to deep  
14 lacustrine turbidite fans, it may reflect an important difference in the type, style and  
15 degree of confinement compared to deep-marine systems.

16 Deep-lacustrine turbidites form important target reservoirs within the North Falkland  
17 Basin (NFB; Richards et al., 2006). The Sea Lion Fan was drilled as an exploration  
18 target by Rockhopper Exploration in 2010 resulting in the discovery of the Sea Lion  
19 Field. The Sea Lion Fan (also referred to as the Sea Lion Complex or Sea Lion Main  
20 Complex) has since been studied by various authors, resulting in a number of  
21 publications that examine aspects of fan distribution and reservoir architecture (Bunt,  
22 2015; Griffiths, 2015; MacAulay, 2015; Williams, 2015; Williams and Newbould,  
23 2015). This paper presents an integrated subsurface study that utilises core, wireline  
24 logs, seismic cross sections and seismic amplitude extraction maps to examine the  
25 deep-lacustrine fans in the North Falkland Basin, with the aim of answering the  
26 following questions: (i) What is the style and character of deposition within deep-  
27 lacustrine fans? (ii) What is the role of partial confinement in controlling lacustrine  
28 systems? (iii) How may this impact hydrocarbon reservoir modelling and  
29 development? (iv) How might lacustrine fans differ from their marine counterparts? In  
30 answering these questions and drawing on the observations and learnings from the  
31 description of the Sea Lion Fan, this paper provides a model for deposition within  
32 deep-lacustrine, partially confined turbidite fans, in general.

## **GEOLOGICAL BACKGROUND**

The Falkland Islands and territorial waters (Fig. 1) are located around 300 km to the south-east of South America. The islands are surrounded by five Mesozoic-aged offshore basins: the South Falkland, Fitzroy, Volunteer, Malvinas and the North Falkland Basin (NFB). The NFB is a failed rift system (Richards et al., 1996a and 1996b), comprising a series of offset depocentres that are affected by two dominant structural trends: North-to-South oriented faulting is predominant in the northern NFB, whereas north-west to south-east oriented faults dominate the southern NFB. This study focuses on the northern portion of the NFB.

The northern extent of the basin has a half-graben geometry (Fig. 2), with major faults on the eastern margin that influenced deposition (Richards et al., 1996a and 1996b; Richards and Fannin, 1997; Richards and Hillier, 2000a; Lohr and Underhill, 2015). From the most-northerly limit to the southern edge, the entire NFB is approximately 250 km long and 100 km wide (from west to east). Rifting is likely to have initiated in the very latest Jurassic or early Cretaceous, with the NFB forming as a failed-rift arm associated with the opening of the South Atlantic (Richards et al., 1996). This rifting phase was then followed by a subsequent thermal sag phase that began in Berriasian-Valanginian times and continued under predominantly continental lacustrine deposition until Albian-Cenomanian times (Fig. 3), when the basin began to develop increasingly marine conditions (Richards et al., 1996a and 1996b; Richards and Fannin, 1997; Richards and Hillier, 2000a).

Up to 1,150 m of late Jurassic to early Cretaceous lacustrine claystones were deposited during the syn-rift and earliest post-rift stages of basin development (Richards and Hillier, 2000b). The thickest, most laterally extensive of these claystones were deposited during the early post-rift phase in Berriasian to early Aptian times (Fig. 3). These lacustrine claystones are organic-rich (up to 7.5% total organic content) and form the principal source rock for discovered hydrocarbons to date (Richards and Hillier, 2000a; 2000b). The early post-rift phase was dominated, at least in the northernmost part of the basin, by the southwards, axial progradation of a lacustrine deltaic system. The progradation of the deltaic units occurred contemporaneously with the deposition of easterly derived, slope apron fans, resulting in a complex inter-fingering of the systems within the basin centre. Five

1  
2  
3 1 separate phases of delta progradation and retreat or hiatus have been identified,  
4 2 additionally several lowstand phases have been mapped as regionally significant  
5 3 unconformities within the basin (Richards and Hillier, 2000a). The base of tectono-  
6 4 stratigraphic unit LC3 (Figs 2 & 3) represents one of these deltaic lowstand-  
7 5 associated unconformities. The LC3 unconformity represents the seismically defined  
8 6 surface onto which the partially confined, slope apron turbidite sediments of the Sea  
9 7 Lion Fan were deposited.

10  
11  
12 8 Several fans, including the Sea Lion Fan have been identified in the LC3 unit  
13 9 (Richards et al., 2006), which were subsequently imaged on a modern, more  
14 10 extensive 3D seismic dataset, and later drilled as part of Rockhopper's 2010  
15 11 exploration campaign (MacAulay, 2015). Here we use the BGS genetic terminology  
16 12 that relates fans and lobes to the location of sediment entry points along the basin  
17 13 margin.

## 14 **METHODS AND DATASETS**

15  
16 15 Over 4,500 km<sup>2</sup> of 3D seismic reflectivity data were acquired over the northern part  
17 16 of the NFB between 2007 and 2011. In 2012, three of the seismic surveys collected  
18 17 during this period were merged to form a single seismic volume. This study makes  
19 18 use of the merged, full-stack 3D volume, which has undergone Kirchhoff, pre-stack  
20 19 time migration and spectral broadening. The polarity of this data is zero phase  
21 20 European (SEG reversed polarity) and is displayed as such in all seismic cross  
22 21 sections in this paper.

23  
24  
25 22 Thirteen exploration/appraisal wells were drilled in the NFB in 2010-2011, nine of  
26 23 which penetrated the Sea Lion Fan. Seven of the nine wells were extensively cored  
27 24 in reservoir-prone sections, with over 455 m of conventional core recovered; all nine  
28 25 wells were logged with a comprehensive suite of wireline surveys undertaken. The  
29 26 455 m of core has been logged at a scale of 1:10 cm to capture information on grain  
30 27 size, lithology and sedimentary structures. Cores have been sampled from the  
31 28 proximal, medial and distal deposits of the Sea Lion Fan, thereby providing sufficient  
32 29 geographical distribution of data.

1 Initial interpretations to build a depositional framework focussed on the  
2 identification of fans as imaged on seismic reflection profiles. Once the individual  
3 fans and lobes had been identified and their distributions mapped on seismic  
4 sections within the 3D volume, a series of seismic reflection amplitude extraction  
5 maps were produced. The amplitude extractions were compiled by extracting  
6 average seismic amplitudes from a +/- 10 millisecond window above and below the  
7 mapped horizon. The resultant aerial distributions of amplitudes were plotted as  
8 colour displays, with variations in amplitude interpreted as representing depositional  
9 trends related to bulk lithological variations, with consideration for the effect of fluid  
10 fill on seismic amplitudes being made. The amplitude maps were then compared  
11 with facies data derived from cores and wireline logs, in order to ground-truth the  
12 lithological interpretations derived from the interpreted amplitude anomalies (Fig. 5).  
13 From this integrated data, a set of facies distribution maps for each fan and lobe  
14 were compiled. Biostratigraphical data was collected from all nine wells that  
15 intersected the Sea Lion Fan, the results of which are addressed in Holmes et al.  
16 (2015).

17 An acknowledgement is made that at the depth and scale of seismic resolution it is  
18 possible that a combination of seismic tuning effects (Simm and Bacon, 2014;  
19 Francis et al., 2015) and variations in fluid fill, may boost the observed amplitude  
20 anomalies. Thin bed tuning may be useful as it is controlled by variations in  
21 sedimentary body thickness, which is principally controlled by sedimentological  
22 processes. The seismic architectures observed in the amplitude extractions appear  
23 well-defined and are comparable in geometry to natural depositional features  
24 observed elsewhere (Adeogba et al., 2005; Fonnesu, 2003; Mayall et al., 2006 and  
25 2010; Posamentier and Kolla, 2003; Prather et al., 1998a).

### 26 ***Turbidite Fans: The Sea Lion North, Sea Lion and Otter Fans***

27 The turbidite fans within this study include: the Sea Lion North Fan, the Sea Lion  
28 Fan and the Otter Fan. The fans are represented by relatively subtle features on  
29 seismic sections, being characterised by both isolated and overlapping, relatively  
30 high-amplitude zones between continuous, lower amplitude seismic reflectors (Fig.  
31 4). The Sea Lion Fan entered the basin from the Sea Lion feeder channel (Fig. 4). It  
32 is composed of three constituent lobes: Sea Lion 10, Sea Lion 15 and Sea Lion 20.

1 The Sea Lion North Fan is younger than the Sea Lion Fan, entering the basin from a  
2 more-northerly located feeder channel, whilst the Otter Fan was likely  
3 penecontemporaneous with the deposition of the Sea Lion Fan, entering the basin  
4 from a more-southerly located feeder channel.

## 5 ***FACIES ANALYSIS***

6 Twelve facies have been identified in the cores from the Sea Lion Fan (Table 1).  
7 These have been grouped into five facies associations representing similar  
8 depositional processes and settings (Fig. 6), which have been recognised in cores  
9 and interpreted in conjunction with a series of seismic amplitude maps (Fig. 7).  
10 These amplitude maps indicate the presence of features interpreted as lobe axis,  
11 lobe fringe and lobe distal fringe deposits, alongside other significant features and/or  
12 processes, including: feeder systems, flow deflection, flow constriction, sinuous lobe  
13 axis deposits, terminal mouth lobes and stranded lobe fringe areas.

14 The Lobe Axis facies association (Fig. 6i), the Lobe Fringe facies association (Fig.  
15 6ii) and the Lobe Distal Fringe facies association (Fig. 6iii) can be used to  
16 characterise the three major elements of any lobe in the fan system, the terminology  
17 for which has been adopted from Prelat et al., (2009). The Hemi-Limnic Mudstones  
18 facies association (Fig. 6iv) represents the background sedimentation (suspension  
19 fall-out) within the lake. The Deformed Sandstones and Mudstones facies  
20 association (Fig. 6v) is interpreted as the product of dewatering or slumping of wet  
21 sediment immediately before or in-between periods of fan activity. In addition, Hybrid  
22 Event Beds are encountered in many of the cores (HEB; Fig. 6vi), typically found in  
23 combination with the Lobe Fringe facies association

### 24 **Lobe Axis Facies Association**

#### 25 Description

26 This facies association (Fig. 6i) comprises fine to coarse grained, well to very well  
27 sorted, structureless sandstone (*fss*), parallel-laminated sandstone (*fpls*), mud-clast  
28 rich sandstone (*fmcs*), rafted mudstone clast-rich sandstone (*frms*) and graded  
29 structured sandstone (*fgss*; Table 1). The lobe axis facies association represents the  
30 dominant cored component within the Sea Lion Fan.

1 Up to 95% of the total thickness of each unit of the facies association is composed of  
2 beds of *fss* (Fig. 8a) which have sharp (non-erosional) contacts at the bed base (Figs  
3 8b & 8c) and occasionally exhibit dish/dewatering structures (Fig. 8d). Beds  
4 dominated by *fss* sometimes exhibit normal grading, parallel laminations and an  
5 increase in the proportion of argillaceous material in the uppermost part of the bed.  
6 Successive beds are mostly amalgamated but may be separated by an intervening  
7 mudstone. Individual beds range between 0.5 - 2 m in thickness and can be found in  
8 amalgamated packages reaching up to 15 m. In addition, there are common  
9 examples of 5-10 cm long, flattened, lithic-clast-armoured, angular mud clasts within  
10 facies mud-clast rich sandstone (*fmcs*, Table 1). These are typically concentrated in  
11 banded horizons in the middle or uppermost part of the beds dominated by *fss*.

### 12 Interpretation

13 The lobe axis facies association, represents deposition predominantly from high  
14 density turbidity currents in which high sediment concentration promoted deposition  
15 of structureless sandstone, dewatering and suppression of near-bed turbulence such  
16 that tractional sedimentary structures are subordinate. (Lowe, 1979; Haughton et al.,  
17 2009). The more fluidised versions of the flow, comprising dewatered, structureless  
18 sandstones (Fig. 6i) are not thought to be very effective at carrying sediment over  
19 long distances (Mutti, 1992). Amalgamated beds of *fss* along with the presence of  
20 *fmcs*, represents periods of erosion, indicating the presence of high energy flows  
21 operating in these locations.

22 The mud clasts present within these deposits were likely ripped-up and entrained in  
23 the flow from a location on the slope and were later deposited on the basin floor in a  
24 concentrated layer, forming at the boundary between a highly concentrated, non-  
25 turbulent carpet and an overlying turbulent layer (Postma et al., 1988). This transition  
26 marks the point where the buoyancy of the less-dense mud clasts and the flow  
27 velocity no longer supported their transport, resulting in deposition. The recognition  
28 of these features and their positioning within the bed is important as they indicate  
29 that at some point the flow was more erosional (Mutti & Nilsen, 1981; Haughton et  
30 al., 2003; Fonnesu et al., 2016).

### 31 **Lobe Fringe Facies Association**

### Description

The lobe fringe facies association (Fig. 6ii) displays beds with more internal structuring including: very fine to fine grained, well sorted *fss*, ripple cross laminated sandstone (*frxls*), *fpls*, inter-bedded sandstone and mudstone (*fism*) and parallel-laminated mudstones (*fplm*; Table 1). Beds tend to be significantly thinner (10 cm to 1 m), exhibit stronger normal grading, and have a greater thickness of structured sandstone facies (*frxls*, *fplm*) above the *fss* at the base of the bed compared to those of the lobe axis facies association. Beds are also less amalgamated and are thus often separated by 10-20 cm thick beds of *fplm*.

### Interpretation

The increased occurrence of structures indicative of more dilute turbulent flow behaviour in the lobe fringe facies association, accompanied by the lowest occurrences of bed amalgamation (i.e. preservation of *fplm* and mudstone caps), thinner bedding, and finer grain size indicates a lower energy depositional environment located adjacent to the lobe axis. The upper-most, represented by *fism*, along with thickly bedded *fplm*, indicates periods of inactivity within the fan. In addition, a lack of evidence for channelization, in the form of inclined erosional surfaces or mud-clast rich, tractional lags at bed bases, helps support deposition within a lobe setting, opposed to a channelized setting.

Lobe fringe areas form a relatively low percentage of the aerial distribution within the Sea Lion Fan, especially compared to lobe axis deposits (Fig. 7). This is because the fans are relatively narrow, perhaps as a result of the constraints imposed by deposition within relatively narrow depressions formed adjacent to preceding deposits (partial confinement), and the fact that the branching, sand-rich systems therefore occupy much of the limited depositional space, preventing the widespread development of lobe fringe deposits. This narrowing of the facies belts along the elongated, partially confined lobes may result in abrupt facies variability internally within compensationally-stacked fan systems.

## **Lobe Distal Fringe Facies Association**

### Description

1 The lobe distal fringe facies association (Fig. 6iii) is characterised by a succession  
2 of thinly-bedded (10-50 cm), well sorted, very fine to fine grained, structureless  
3 sandstone (*fss*), followed vertically by well-developed ripple-cross laminated  
4 sandstones (*frx/s*) and parallel-laminated mudstones (*fplm*) (Table 1; Fig. 8i). In  
5 general, mud clast are absent from this facies association. This facies association  
6 can be found in proximal, medial and distal parts of the Sea Lion Fan. The proximal  
7 version of the lobe distal fringe deposits are represented in core from well 14/10-5 in  
8 the Sea Lion 10 lobe (Fig. 8i; Fig 11). The medial versions of the lobe distal fringe  
9 are observed in SL20 in well 14/10-6 (Fig 8iii; Fig.11) and are represented by a  
10 succession of *fss* and *frx/s*, but with thicker interbeds of *fpls* and *fplm*. The presence  
11 of *fpls* and *fplm*, along with reduced bed amalgamation, provides a strong indication  
12 for a fringing location (Romans et al., 2009). To date, there is no core data from the  
13 distal versions of the lobe distal fringe facies of the Sea Lion Fan.

#### 14 Interpretation

15 These deposits are interpreted to be the product of fully turbulent, low-density  
16 turbidity currents (Lowe, 1979; Haughton et al., 2009). They can be formed by the  
17 reduction of sediment concentration through prior deposition and flow run out into  
18 the lobe distal fringe locations. The presence of low-density turbidite structures in  
19 well sorted, very fine grained sandstones, in extremely proximal, lobe distal fringe  
20 locations indicates that flow transformation occurred abruptly, laterally away from the  
21 main depositional lobe axis, and not just through down-dip progression in the distal  
22 fan. This has lead to vertical stacking of low-density turbidites. The thin-nature (1-2  
23 cm) of capping beds of hemi-limnic mudstones (Fig. 8i) is interpreted to be a  
24 function of consistent activity of the adjacent lobe axis/lobe fringe setting and  
25 continued delivery of dilute(ed) turbidites into the lobe distal fringe areas, restricting  
26 the deposition of thickly-bedded hemi-limnic mudstones. Medial versions of the lobe  
27 distal fringe represent similar depositional processes, but contain more thickly  
28 developed, hemi-pelagic mudstones, representing longer breaks in sediment delivery  
29 to these locations, in comparison to the proximal locations.

30 For the Sea Lion Fan model, proximal and medial versions of the lobe distal fringe  
31 have been used as analogues for anticipated sedimentology found in the distal  
32 reaches of the fan. In the distal areas, more thinly bedded, finer grained versions of

1 the lobe distal fringe are envisaged. These deposits are expected to contain thicker,  
2 more regular units of *fplm*, interspersed between the lower density turbidite deposits,  
3 representing periods of fan inactivity.

#### 4 **Hemi-Limnic Mudstones Facies Association**

##### 5 Description

6 The hemi-limnic mudstones facies association (Fig. 6iv) comprises 0.01-8 m thick  
7 units of *fplm* (Table 1.) They are inter-laminated with sparse, silt-grade laminae,  
8 contain little evidence for bioturbation and otherwise are homogeneous except for  
9 occasional 1-8 cm thick, light grey to orange coloured, siliceous intervals of clay-  
10 grade material.

##### 11 Interpretation

12 These deposits represent the background, hemi-limnic sedimentation of the  
13 lacustrine environment, with seasonal variations in productivity forming the  
14 laminations (Anderson and Dean, 1988). The light grey to orange coloured, siliceous  
15 intervals are interpreted as tonstein bands, deposited through volcanic ash-fall into a  
16 standing body of freshwater, typically described in coalfield successions (Spears,  
17 2012).

18 As lacustrine deposition is relatively slow and constant, units of hemi-limnic  
19 mudstones can be used as an indication of the general activity or inactivity of each  
20 fan and lobe. In a very general sense, thin units of hemi-limnic mudstones represent  
21 breaks in turbidite deposition within one lobe, whereas significantly thicker units  
22 (perhaps >0.5 m) demonstrate major regional breaks in coarser-grained clastic  
23 deposition, potentially linked to fan de-activation and abandonment.

#### 24 **Deformed Sandstones and Mudstones Facies Association**

##### 25 Description

26 The deformed sandstones and mudstones facies association (Fig. 6v) represents  
27 packages comprised of well sorted, fine-grained sandstones, intercalated with  
28 siltstones and mudstones (Fig.10). They range from 0.05 to 3 m in thickness and are  
29 present as both relatively isolated occurrences or as thick intervals of disruption.  
30 Examples of deformed sandstones and mudstones can be found throughout the Sea

1  
2  
3 1 Lion Fan, with the best examples observed in the Sea Lion 15 Lobe at the 14/10-7  
4 2 well location (Fig. 7c).

6  
7 3 Interpretation

8 4 The chaotic intercalation of sandstones and mudstones is interpreted to have been  
9 5 caused by a combination of: heavy dewatering; remobilisation of sandstones; and  
10 6 slumping or sliding. Features produced during dewatering include small mud/sand-  
11 7 volcanoes (Fig. 10a). In this example, primary fabrics have undergone a c. 90°  
12 8 rotation, indicating significant localised deformation and re-mobilisation. The  
13 9 arrangement of the facies makes it difficult to determine any defining facies evolution  
14 10 or succession; much of the original, primary depositional structure has been  
15 11 disrupted. It is possible that some of the isolated occurrences (Fig. 10b) may  
16 12 represent the product of hybrid event beds formed by substrate de-lamination  
17 13 (Fonnesu, et al., 2016).

25  
26 14 **Hybrid Event Beds (mixed flow behaviour) – A Bed Type**

27 15 Hybrid Event Beds represent the deposits of flows that exhibit mixed flow behaviour  
28 16 and are considered as a “bed type” in the model for the Sea Lion Fan. They are  
29 17 observed in association with lobe fringe deposition, but theoretically should also be  
30 18 found alongside lobe distal fringe deposits in the medial and distal parts of the fan  
31 19 (Davis et al., 2009). Unfortunately, the medial and distal expressions of the lobe  
32 20 distal fringe facies association are currently un-characterised in core data from the  
33 21 Sea Lion Fan.

39  
40 22 Description

41 23 The hybrid event beds (Fig. 6vi) consist of a lower portion of *fss* overlain by a  
42 24 succession of argillaceous breccias (*fab1-3*; Table 1). Internally, the upper portion of  
43 25 the facies association is composed of three successive facies (*fab1-3*). These  
44 26 argillaceous facies typically exhibit sharp basal contacts, with the argillaceous matrix  
45 27 component of each successive facies increasing upwards above the sharp  
46 28 boundaries (Fig. 9). Facies *fab1* and *fab2* commonly display elongate, 1-5 cm long  
47 29 mud-clasts. In *fab3*, the larger mud-clasts have been replaced by a concentration of  
48 30 carbonaceous material in the matrix. These deposits are encountered in wells from  
49 31 the medial part of the Sea Lion Fan, in lobe fringe locations (SL15 in 14/10-6 and  
50  
51  
52  
53  
54  
55  
56  
57  
58  
59  
60

1 14/10-7). In distal locations, they were not observed in the deposits of the lobe axis  
2 facies association (in 14/15-4Z) and there are currently no well penetrations through  
3 the lobe fringe or lobe distal fringe in this part of the fan.

#### 4 Interpretation

5 This bed type represents the deposits of flows that exhibit evidence for mixed flow  
6 behaviour (Haughton et al., 2009 and Kane and Pontén, 2012). In the Sea Lion Fan,  
7 they have been observed in two examples from the SL15 lobe, in 14/10-6 and 14/10-  
8 7 (Fig 11.) In Haughton et al. (2009), these deposits are referred to as “hybrid event  
9 beds” and have been described in detail in, among many other examples, the deep-  
10 marine sediments of the North Sea (Barker et al., 2008; Davis et al., 2009; Haughton  
11 et al., 2003; 2009); in the North Apennine Gottero Sandstone, north-west Italy  
12 (Fonnesu et al., 2015; 2017); the Springar Formation, Voring Basin, Norwegian  
13 North Sea (Southern et al., 2017); and the Marnoso Arenacea Formation, Italy (Amy  
14 and Talling, 2006).

15 The alternative model for the formation of hybrid beds, through relatively distal flow  
16 transformation, is presented in Kane et al., (2017). These have been referred to as  
17 transitional flow deposits in examples from the Gulf of Mexico (Kane and Pontén,  
18 2012). The main difference between the two models is that the basal, structureless  
19 sandstone represents the product of distal flow collapse, as opposed to the product  
20 of a forerunning turbidity current (*sensu* Haughton et al., 2003; 2009). For the Sea  
21 Lion Fan, it is difficult to completely discount either model given the limited number of  
22 examples observed in core data, but we prefer to use the HEB terminology for the  
23 purposes of this study.

24 The basal unit of *fss* is interpreted to have been deposited rapidly, under a non-  
25 cohesive, high-density turbidity current and corresponds to “H1” in Haughton et al.,  
26 (2009). The upper section, representing the *fab1-3* succession, was deposited under  
27 turbulence-suppressed, more cohesive conditions, facilitated by an argillaceous, finer  
28 grained component in the flow (Baas et al., 2009). The *fab1-3* sequence (Table 1;  
29 Fig. 9) represents the “debritic” portion of the hybrid event bed. These deposits are  
30 interpreted as hybrid event beds, which were the product of a single flow event

1  
2  
3  
4  
5  
6  
7  
8  
9  
10  
11  
12  
13  
14  
15  
16  
17  
18  
19  
20  
21  
22  
23  
24  
25  
26  
27  
28  
29  
30  
31  
32  
33  
34  
35  
36  
37  
38  
39  
40  
41  
42  
43  
44  
45  
46  
47  
48  
49  
50  
51  
52  
53  
54  
55  
56  
57  
58  
59  
60

1 undergoing flow-partitioning during downslope evolution, resulting in a flow which  
2 displays mixed behaviour (Haughton et al., 2003; 2009).

3 Internally, sharp jumps in argillaceous matrix content across the *fab1-3* boundaries  
4 are observed (Fig. 9). This may indicate further segregation or abrupt switches in  
5 flow rheology occurring within an already partitioned flow, alternatively these  
6 deposits could represent the product of transitional flows (Kane and Pontén, 2012).  
7 *Fab1* represents the lower most bed and can be equated to “H2” in Haughton et al.  
8 (2009), whereas the overlying *Fab2* can be equated to “H3”. The “H3” bed has since  
9 been further subdivided into six categories, termed “HEB 1-6” (Fonnesu et al., 2017).  
10 Lateral variability in H3 can be used to determine the processes which introduced  
11 fine grained material into the flow, whether it be up-dip turbulent erosion on the shelf;  
12 or substrate de-lamination in the basin (Fonnesu et al., 2016; 2017).

13 *Fab3* is interpreted as representing the product of deposition out of suspension  
14 rather than forming part of the cohesive flow, with the loss of energy allowing the fine  
15 grained, light carbonaceous grains to settle and therefore concentrate. An alternative  
16 interpretation might be presented where the carbonaceous grains have been  
17 accumulated through longitudinal fractionation of the lighter components of the flow  
18 (Haughton et al., 2009). However, the relatively short transport distances in the Sea  
19 Lion Fan (5-10 km) may not permit efficient development of longitudinal segregation  
20 of fine-grained material. In some of the examples, *fab3* is absent (Fig. 9), which is  
21 probably a result of the original flow composition not containing much in the way of  
22 late-stage suspension material, resulting in poor perseveration of this upper facies.  
23 The *fab3* facies is distinct from “normal” background settling as the water column has  
24 been disrupted and contains fines, such as carbonaceous material, that do not  
25 represent standard fall-out within the lacustrine environment.

## 26 **SEISMIC AMPLITUDE ARCHITECTURES**

27 Three sediment entry points, identified in 3D seismic data, along the eastern margin  
28 of the NFB are associated collectively with three fans, which can be subdivided into  
29 a total of six different individual lobes (Fig. 7). The “fan” and “lobe” nomenclature has  
30 been applied and refers to a single fan in which there are multiple lobes that are fed  
31 from one common, linked feeder system. Each of the three fans, and the lobes within

1 the fans, display compensational-offset stacking (Fig. 4). Internally, within individual  
2 lobes, architectures are observed in seismic amplitude extraction maps (Fig. 7). The  
3 seismic amplitude architectures include: feeder systems, terminal mouth lobes, flow  
4 deflection, sinuous lobe axis deposits, flow constriction and stranded lobe fringe  
5 areas.

### 6 **Feeder Systems**

7 These features (Figs 7b, 7c & 7d) are observed as narrow (100 m – 300 m wide),  
8 downslope-widening, bright anomalies at the heads of fans and record the positions  
9 of sediment entry at the base of slope. The feeder systems appear to be detached  
10 from the up-slope areas, likely facilitated by slope bypass by the turbidite currents  
11 (Mutti et al., 1994, 2003; Stevenson et al., 2015). The detachment of the feeder  
12 systems from the slope margin is likely responsible for the successful up-dip  
13 stratigraphic sealing of the Sea Lion oil discovery.

### 14 **Terminal Mouth Lobes**

15 Terminal mouth lobe architectures (Figs 7b & 7d) are commonly observed in the  
16 medial-to-distal fan. These are represented in amplitude extraction maps as bright  
17 amplitudes with fanning-outwards geometries around 1.5 km in width. The well-  
18 defined, lateral limits of the bright amplitudes are coincident with the abrupt pinch-out  
19 of that seismic reflector (Fig. 7b). The terminal mouth lobes are dominated by  
20 stacked deposits of the lobe axis facies association. These are interpreted as the  
21 product of flows which may have bypassed the proximal-to-medial part of the fan,  
22 carrying coarse grained material into the distal part of the system. Bypass may have  
23 been enhanced by the partial confinement and elongation of the system, which acted  
24 to constrain the flow pathway, resulting in continuing delivery of fine-to-medium  
25 grained sand to the distally located terminal mouth lobes. The continuous delivery of  
26 sand to these locations is evidenced by bed amalgamation and the lack of  
27 development of intervening *fplm* in these locations (and dominance of lobe axis  
28 facies).

### 29 **Flow Deflection**

30 There are a few examples of flow deflection of one or more lobes by pre-existing  
31 palaeo-bathymetric highs. The highs are interpreted to be associated with earlier fan

1  
2  
3 1 deposition, which may have acted to constrain the bed-to-lobe element scale (Prelat  
4 et al., 2009) fan and lobe deposits. Figure 7c illustrates the deflection of flows within  
5 2 the SL15 lobe by deposits of the older, pre-existing Sea Lion North fan (SLN). The  
6 3 similarity in size between each fan is an important factor to consider when examining  
7 4 flow deflection as this is likely to provide some control on whether flows surmount  
8 5 topography associated with the fan or are deflected by it.  
9 6  
10 7  
11 8  
12 9  
13 10  
14 11  
15 12  
16 13  
17 14  
18 15  
19 16  
20 17  
21 18  
22 19  
23 20  
24 21  
25 22  
26 23  
27 24  
28 25  
29 26  
30 27  
31 28  
32 29  
33 30

### 7 **Sinuuous Lobe Axis Deposits**

8 Sinuous lobe axis deposits are widely recognised on the amplitude maps from all of  
9 the fans and lobes (Fig. 7). They form very bright, high amplitude, relatively narrow  
10 features (approximately 100-1000 m wide) that extend basinwards for several  
11 kilometres. They are gently sinuous in nature and sometimes exhibit branching (Fig.  
12 7d). The sinuous forms are oriented parallel to the main elongation axis of the fan,  
13 along the direction of flow from the confined feeder channels in the east, to the basin  
14 centre in the west. They have been cored in SL20 in 14/10-5 (Fig. 11) and are  
15 dominated by less well sorted examples of the lobe axis facies association, which  
16 typically exhibit *frms*, particularly at bed tops.  
17  
18  
19  
20  
21  
22  
23  
24  
25  
26  
27  
28  
29  
30  
31  
32  
33  
34  
35  
36  
37  
38  
39  
40  
41  
42  
43  
44  
45  
46  
47  
48  
49  
50  
51  
52  
53  
54  
55  
56  
57  
58  
59  
60

### 17 **Flow Constriction**

18 Flow constriction of the lobe axis deposits has been observed, particularly in medial  
19 to distal locations (Fig. 7b). These features are interpreted to represent areas where  
20 the flow was being focussed, either as a result of passing between palaeo-  
21 bathymetric highs (e.g. Davis et al., 2009) or due to local increases in substrate  
22 gradient and subsequent incision of conduits that were eventually filled (Kneller,  
23 2003). The flow constriction and down-flow branching may reflect flow transformation  
24 from high-density flow, to lower-concentration, less turbulent flows in the down-dip  
25 locations (Kneller, 2003). An alternative interpretation is possible, where such forms  
26 represent the neck of lobe deposits, which formed immediately down-dip from a zone  
27 of bypass across the fan surface (Fonnesu, 2003). In the Sea Lion Fan, there is no  
28 representative core through an area of flow constriction, limiting the interpretation of  
29 depositional processes at these sites.  
30  
31  
32  
33  
34  
35  
36  
37  
38  
39  
40  
41  
42  
43  
44  
45  
46  
47  
48  
49  
50  
51  
52  
53  
54  
55  
56  
57  
58  
59  
60

### 30 **Stranded Lobe Fringe Areas**

1  
2  
3 1 Stranded lobe fringe areas, largely comprising deposits of the lobe fringe facies  
4 2 association, are recognised in all of the individual lobes comprising Sea Lion as  
5 3 relatively low amplitude zones separating sinuous lobe axis deposits (Fig. 7d). These  
6 4 are most pervasive in the medial parts of each fan. The stranded lobe fringe areas  
7 5 are distinct from surrounding mudstone dominated, basin-floor areas (e.g. outside  
8 6 the fan system).

## 7 ***DISCUSSION***

### 8 **Style, character and controls on deposition within the Sea Lion Fan**

9 Seismic correlation and mapping of amplitude extractions and facies association  
10 distributions has facilitated the delineation of depositional facies zones across the  
11 Sea Lion 10, Sea Lion 15 and Sea Lion 20 lobes of the Sea Lion Fan (Figs 7 & 11).  
12 Each of the lobes has a proximal to distal elongated geometry, with lobe lengths  
13 approximately three times greater than their widths (13 km long vs. 4 km wide). The  
14 composite lobes are therefore relatively linear, and exhibit more restricted outwards  
15 spreading geometries than those observed in many deep-water marine systems  
16 (Richards et al., 1998; Stow and Mayall, 2000; Mayall et al., 2006; 2010). The overall  
17 north-south elongated shape of the palaeo-bathymetry and the limited size of the  
18 basin is interpreted to have exerted some control on the axial nature of these  
19 features, with the fans flowing towards the deepest parts of the basin in the south.

20 The Sea Lion Fan accords with the “line-sourced, sand rich, slope apron fan”  
21 category of submarine fan types identified by Richards et al. (1998). Such features  
22 are usually small in terms of relative spatial distribution, have moderate to high slope  
23 gradients, a linear belt shape extending 1-10 km and a small, narrow shelf area. The  
24 high degree of sorting, as well as the presence of berthierine-coated grains (ooids)  
25 and pelletal glauconite within the turbidites have been used as evidence to suggest  
26 that they were fed from over-steepened, fringing lacustrine beach bars (Williams,  
27 2015). These fringing beach bars may have been present along the basin margin  
28 (Figs 12 & 13), where the sediments were pre-sorted. The fringing shelfal clastics  
29 built up into beach deposits along the margin, until they became unstable and failed  
30 or were eroded into during episodic wetter periods (Fig. 14). This occurred at a  
31 number of different sediment feeder points located along the basin margin (e.g. Sea  
32 Lion North feeder, Sea Lion feeder and Otter feeder, Fig. 12).

1  
2  
3 1 Some of these feeder points supplied only one fan (the Sea Lion North Fan),  
4 2 whereas others were longer lived and were the site of multiple fan development (the  
5 3 Otter Fan and the Casper Fan, discussed in Bunt, 2015). Reasons why some fan  
6 4 feeders display relative longevity in terms of supplying multiple, temporally spaced  
7 5 fans to the basin whilst others supplied single fans are challenging to resolve with  
8 6 the existing data. One plausible explanation may be that river systems in the  
9 7 hinterland brought sediment into the fringing littoral system, which may have been  
10 8 re-worked and piled-up at specific locations, perhaps in areas where the shelf was  
11 9 slightly wider. This was then available to feed the deep-lacustrine fans through  
12 10 failure by over-steepening or re-working during down-cutting lowstand events. This  
13 11 re-use of sediment entry points, implies that basin-margin geometries and hinterland  
14 12 drainage systems may have exerted a large control on the loci of turbidite fan input  
15 13 along the eastern margin. At a regional scale, the Sea Lion Fan forms only one part  
16 14 of a series of southerly migrating fans arranged in a compensational-offset stacking  
17 15 pattern (Fig. 4). Input of sediment was controlled by the southerly prograding delta  
18 16 that successively shut down these fans by choking the feeder systems (Fig. 14).

19  
20  
21  
22  
23  
24  
25  
26  
27  
28  
29  
30 17 The triggering mechanism for the multi-phased delivery of sand into the NFB is still  
31 18 uncertain. Line-sourced, sand rich, slope apron fans tend to form predominantly  
32 19 during relative falls of base level, even though effective control of relative water level  
33 20 positions in terms of cycles and systems on the development or initiation of  
34 21 lacustrine fans is of low importance (Richards and Bowman, 1998). Many of the fans  
35 22 described above down-lap onto a regional unconformity surface (base of unit LC3 of  
36 23 Richards and Hillier, 2000a), which defines a significant hiatus in the southwards  
37 24 axial progradation of a major delta into the lacustrine basin during the early  
38 25 Cretaceous. Such relative falls of base level could have been triggered by faulting  
39 26 associated with regional uplift along the basin margin, causing lowering of the basin  
40 27 floor and sediment instability along the fringing shelf, resulting in the generation of  
41 28 the turbidite flows.

42  
43  
44  
45  
46  
47  
48  
49  
50  
51 29 However, many of the fans within LC3 are underlain by at least one similar fan,  
52 30 developed below the LC3 unit's lower boundary as described in Lohr and Underhill  
53 31 (2015). These earlier fans have similar elongated, north-west/south-east oriented  
54 32 geometries to the fans within LC3. This implies that the mechanism controlling the

1 origin and evolution of fans along the basin margin was operating prior to full-scale  
2 development of low-stand conditions in the basin coincident with major delta hiatus.  
3 Further discussion on the influence of basin margin geometries on sediment input  
4 along the eastern margin of the NFB can be found in Lohr and Underhill (2015).  
5 Fault geometry and activity at the basin margin is likely to have exerted a control on  
6 the position of the sediment entry points into the basin, providing discontinuities for  
7 the hinterland's drainage pathways (Lohr and Underhill, 2015). Richards et al. (2006)  
8 suggested that relay ramps along the basin margin may have provided sediment  
9 entry pathways for fan development into the basin. The Sea Lion Fan and Otter Fan  
10 feeders have similar orientations to the Sea Lion North Fan feeder channel, but  
11 display no corresponding evidence of underlying, controlling fault systems cross-  
12 cutting the basin margin fault. The point of maximum throw on the basin margin  
13 faults do not seem to coincide with the position of sand entry points along the  
14 margin. After entering the basin roughly perpendicular to the margin, the fans instead  
15 swing in a southerly direction, towards the basin's topographically lowest point (Fig.  
16 12).

### 17 **The role of partial confinement in controlling lacustrine systems**

18 This study suggests that evidence for partial confinement of a system is presented  
19 by a combination of the following: sinuous lobe axis deposits, fan elongation,  
20 constriction of flow and flow deflection. The identification of elongated fans is  
21 important as it suggests that: flows were highly efficient, likely by virtue of high  
22 sediment volumes (Al Ja'aidi et al., 2004). The importance of recognising any form of  
23 confinement within a system, in this case partial confinement controlled by flow size  
24 and depositional topography, is that there may be potential for abrupt, lateral facies  
25 variability (as observed in Lomas and Joseph, 2004). When considering a  
26 compensationally stacked succession of turbidite fan and lobe deposits, the  
27 constraint of facies belts along elongated corridors through partial confinement  
28 may result in the aggradation of a highly complex suite of sediments.

29 There are a number of factors that may control partial confinement, including: the  
30 size of the flow and the amount of sediment entering the basin compared with the  
31 scale of the margin; the ability of deposits from preceding flows to control the next  
32 event bed pathway; factors that control flow efficiency, including flow volume and

1 grain size distribution (Al' Jaidi et al., 2004); slope gradient; and a difference in flow  
2 rheology when sediment gravity flows enter a freshwater basin, compared with salt-  
3 water basins.

#### 4 **Effects of heterogeneity on hydrocarbon reservoir modelling**

5 A consideration for the presence of heterogeneities within deep-lacustrine turbidite  
6 fans needs to be made, particularly in light of their increasing exploitation as  
7 hydrocarbon reservoirs. The identification of partial confinement within these  
8 systems suggests that lateral facies variability can be abrupt, facilitated by the  
9 elongation of the fans and constraint of facies belts. The vertical stacking of the  
10 lobes within the fans will lead to a complex facies model, with vertical stacking of  
11 highly variable sub-environments. This study also suggests that a "simple" proximal-  
12 to-distal degradation in reservoir properties will be insufficient for correctly modelling  
13 these systems.

14 One major aspect concerns the distribution of hybrid event beds, which are  
15 observed in association with lobe fringe deposition (Fig. 11) and the potential for  
16 enhanced development of these deposits in the lobe distal fringe. Most studies  
17 demonstrate that hybrid event beds, deposited in deep-marine systems, are mainly  
18 present in the lobe fringe or more distal settings (Haughton et al., 2003; 2009;  
19 Talling, 2013; Kane et al., 2017). For example, hybrid event beds dominate the outer  
20 and distal parts of the Forties Fan of the Central North Sea, in the Everest, Lomond  
21 and Pierce fields (Davis, et al., 2009) and the Permian Skoorsteenberg Formation, in  
22 the Karoo Basin, South Africa (Hodgson, 2009). There are only rare examples where  
23 hybrid event beds are encountered in relation to channels (Terlaky and Arnott,  
24 2014). Hybrid Event Bed deposits formed in lacustrine basins are rarely documented  
25 in the literature (another example being Tan et al., 2017).

26 Hybrid event beds contain elevated fines within the matrix, which greatly reduces  
27 poro-perm characteristics, commonly resulting in these units representing poor  
28 reservoir lithologies (Talling, 2013; Porten et al., 2016). An under appreciation for the  
29 distribution and thickness of these deposits will result in reduced oil reserves and,  
30 perhaps more importantly, these deposits have the potential to form baffles or  
31 barriers within the reservoirs (Amy et al., 2009).

## 1 **Lacustrine Versus Marine Turbidite Systems**

2 It is important to briefly highlight some of the similarities and differences between  
3 lacustrine systems and marine systems. Deep-water sedimentation in both marine  
4 and lacustrine settings appears to be composed of a similar suite of sediments, from  
5 high-density to low-density turbidite deposits, through to hybrid event beds and  
6 background, hemi-limnic deposition; the processes operating in the lacustrine  
7 environment are quite similar. The flows entering the basin form comparable  
8 depositional geometries, with fanning outwards of the systems and compensational  
9 stacking of internal lobes.

10 Some aspects of fan models developed in marine systems are clearly still applicable  
11 to deep-lacustrine basins. In particular, fan architectures of lacustrine turbidite  
12 systems, such as the Sea Lion Fan, may be more comparable to marine turbidite  
13 systems that are affected by confining palaeobathymetry (e.g. Lomas and Joseph,  
14 2004; Amy et al., 2004). Lacustrine turbidite systems, deposited on an enclosed  
15 basin floor, are relatively small compared to that of the overall scale of the margin.  
16 Pre-existing palaeo-bathymetry will therefore be able to fundamentally affect the flow  
17 direction and impose a control over the velocity of the turbidite flows, which in-turn  
18 may modify the resultant depositional geometries produced. The overall geometry of  
19 the basin has a strong influence on focussing the direction of any one, or a set of fan  
20 systems, towards the deepest parts of a lake. This is in contrast to an unconfined  
21 marine setting (Bouma et al., 2012), where lobe distribution remains relatively  
22 unrestricted. In these settings, the size of the fans entering the basin and the volume  
23 of sediment delivery are large, permitting the overriding of palaeobathymetry.

24 When turbidite fans in lacustrine basins are examined at the smaller scale of  
25 individual fans and lobes, feeder systems, sinuous lobe axis deposits and terminal  
26 mouth lobes can be identified. The main control over the constraint of the lobe axis  
27 deposits to sinuous belts is interpreted to be a function of the size of the flow  
28 entering the basin compared to pre-existing palaeobathymetry. Additionally, it is  
29 possible there is a critical difference between the rheology and characteristics of  
30 flows entering saltwater basins (marine) compared to flows entering basins filled with  
31 fresh-brackish water (lacustrine). The difference in fluid infilling these two types of

1 basins may provide another important control on the partial confinement of the  
2 system, resulting in the architectural geometries observed in the Sea Lion Fan.

3 Ancient deep lacustrine turbidite fans are rarely described in the literature, making  
4 the Sea Lion Fan an important starting point in terms of research into deep-lacustrine  
5 fan systems. Given this, a number of major questions should be answered, these  
6 include: is there a difference in flow properties imparted by having a basin filled with  
7 fresh water as opposed to salt water?; Does this result in different styles of flow,  
8 where lobe axis deposits tend to follow more sinuous pathways?; Can this result in  
9 the ability of small variations in palaeo-bathymetry to impart enhanced control on  
10 flow direction? Future studies, such as outcrop studies and lab experiments (lock-  
11 gate), should focus on identifying differences between sediment gravity flows into  
12 fresh water and salt water basins.

### 13 **CONCLUSIONS**

- 14 1. Heterogeneity in lacustrine, partially confined turbidite fans can be modelled  
15 using a combination of amplitude maps, core data and wireline correlations.
- 16 2. Lacustrine fans can be relatively sand rich, but still contain numerous scales  
17 of heterogeneity, including both high and low-density turbidites, hybrid event  
18 beds and re-mobilised/deformed sediments.
- 19 3. Partial confinement of deep-lacustrine systems is evidenced by a combination  
20 of the following architectures: sinuous lobe axis deposits, fan elongation,  
21 constriction of flow and flow deflection.
- 22 4. The presence of hybrid event beds, along with other heterogeneities, have the  
23 potential to form complexity within lacustrine fan hydrocarbon reservoirs.
- 24 5. Deep-water marine and lacustrine environments display a set of sedimentary  
25 processes that form comparable deposits. However, observations of seismic  
26 architectures suggest that lacustrine systems may be more laterally  
27 constrained than compared with marine counterparts.
- 28 6. Lacustrine turbidite systems are likely more similar to confined marine  
29 systems than marine systems un-affected by confinement associated with  
30 seafloor topography.
- 31 7. Outcrop studies are required to characterize the sub-seismic aspects of  
32 lacustrine systems, which could be complemented by lab-testing in the form of

1 lock-gate experiments, designed to examine differences in flow properties of  
2 sediment gravity flows into fresh versus salt water bodies.

### 3 **ACKNOWLEDGEMENTS**

4 Premier Oil and Rockhopper Exploration are thanked for kindly allowing the  
5 publication of commercial well-log, core and seismic data in advance of general  
6 public release. Premier Oil and Rockhopper Exploration stress that “the  
7 interpretations and opinions expressed in this paper are those of the authors and do  
8 not necessarily reflect the interpretations and opinions of the Sea Lion operator and  
9 partners.” We also thank staff from Desire Petroleum and Falklands Oil and Gas for  
10 their constructive comments on an earlier draft of this paper. Ian Andrews, Dave  
11 Schofield, Lucy Williams and Robert Newbould are specifically thanked for their  
12 helpful comments. Sarah Southern and Marco Fonnesu are thanked for their  
13 thoughtful and critical reviews that vastly improved the manuscript. Ian Kane and  
14 Nigel Mountney are thanked for editorial advice. The paper is published by  
15 permission of the Director, Mineral Resources, Falkland Islands Government, and  
16 the Executive Director, British Geological Survey (NERC).

**REFERENCES**

- Adeogba, A.A., McHargue, T.R. & Graham, S.A.** (2005) Transient fan architecture and depositional controls from near-surface 3-D seismic data, Niger Delta continental slope. *AAPG Bulletin*, 89, 5, 627-643.
- Al Ja'aidi, O.S., McCaffrey, W.D. & Kneller, B.C.** (2004) Factors influencing the deposit geometry of experimental turbidity currents: implication for sand-body architecture in confined basins. From: Lomas, S.A. & Joseph, P. (eds) (2004) *Confined Turbidite Systems. Geological Society, London, Special Publication, 222*, 45-58.
- Amy, L. A., McCaffrey, W. D., & Kneller, B. C.** (2004). The influence of a lateral basin-slope on the depositional patterns of natural and experimental turbidity currents. *Geological Society, London, Special Publications, 221(1)*, 311-330.
- Amy, L.A. & Talling, P.J.** (2006) Anatomy of turbidites and linked debrites based on long distance (120-30km) bed correlation, Marnoso Arenacea Formation, Northern Apennines, Italy. *Sedimentology*, 53, 161-212.
- Amy, L.A., Peachey, S.A., Gardiner, A.A. & Talling, P.J.** (2009) Prediction of hydrocarbon recovery from turbidite sandstones with linked-debrite facies: Numerical flow simulation studies. *Marine and Petroleum Geology*, 26, 2032-2043.
- Anderson, R.Y. & Dean, W.E.** (1988) Lacustrine varve formation through time. *Palaeogeography, Palaeoclimatology, Palaeoecology*, 62, 215-235.
- Baas, J.H., Best, J.L., Peakall, J. & Wang, M.** (2009) A phase diagram for turbulent, transitional, and laminar clay suspension flows. *Journal of Sedimentary Research*, 79, 162-183.
- Barker, S.P., Haughton, P.D.W., McCaffrey, W.D., Archer, S.G. & Hakes, B.** (2008) Development of Rheological Heterogeneity in Clay-rich High Density Turbidity Currents: Aptian Britannia Sandstone Member, U.K. Continental Shelf. *Journal of Sedimentary Research*, 78, 45-68.
- Bouma, A. H., Normark, W. R., & Barnes, N. E.** (Eds.). (2012). *Submarine fans and related turbidite systems*. Springer Science & Business Media.
- Bunt, R.J.W.** (2015) The use of seismic attributes for fan and reservoir definition in the Sea Lion Field, North Falkland Basin. *Petroleum Geoscience*, 21, 137-149.
- Crossley, R.**, (1984) Controls on Sedimentation in the Malawi Rift Valley, Central Africa. *Sedimentary Geology*, 40, 33-50.
- Covault, J.A. & Romans, B.W.** (2009) Growth patterns of deep-sea fans revisited: Turbidite-system morphology in confined basins, examples from the California Borderland. *Marine Geology*, 265, 51-66.
- Davis, C., Haughton, P.D.W, McCaffrey, W., Scott, E., Hogg, N. & Kitching, D.** (2009) Character and distribution of hybrid sediment gravity flow deposits from the

- 1  
2  
3 1 outer Forties Fan, Palaeocene Central North Sea, UKCS. *Marine and Petroleum*  
4 2 *Geology*, 26, 1919-1939.  
5  
6 3 **Fonnesu, F.** (2003) 3D seismic images of a low-sinuosity slope channel and related  
7 4 depositional lobe (West Africa deep-offshore). *Marine and Petroleum Geology*, 20,  
8 5 615-629.  
9  
10 6 **Fonnesu, M., Haughton, P.D.W., Felletti, F. & McCaffrey, W.** (2015) Short length-  
11 7 scale variability of hybrid event beds and its applied significance. *Marine and*  
12 8 *Petroleum Geology*, 67, 583-603.  
13  
14 9 **Fonnesu, M., Patacci, M., Haughton, P.D.W., Felletti, F. & McCaffrey, W.D.**  
15 10 (2016) Hybrid Event Beds Generated By Local Substrate Delamination On A  
16 11 Confined-Basin Floor. *Journal of Sedimentary Research*, 86, 929-943.  
17  
18 12 **Fonnesu, M., Felletti, F., Haughton, P.D.W., Patacci, M. & McCaffrey, W.D.**  
19 13 (2017) Hybrid event bed character and distribution linked to turbidite system sub-  
20 14 environments: The North Apennine Gottero Sandstone (north-west Italy).  
21 15 *Sedimentology*, doi:10.1111/sed.12376  
22  
23 16 **Francis, A., Lewis, M., & Booth, C.** (2015) Sea Lion Field, North Falkland Basin:  
24 17 seismic inversion and quantitative interpretation. *Petroleum Geoscience*, 21, 151-  
25 18 169.  
26  
27 19 **Fugitt, D. S., Stelting, C. E., Schweller, W. J., Florstedt, J. E., Herricks, G. J., &**  
28 20 **Wise, M. R.** (2000). Production characteristics of sheet and channelized turbidite  
29 21 reservoirs, Garden Banks 191, Gulf of Mexico, USA. *The Leading Edge*, 19, 4, 356-  
30 22 369.  
31  
32 23 **Griffiths, A.** (2015) The reservoir characterization of the Sea Lion Field. *Petroleum*  
33 24 *Geoscience*, 21, 199-209.  
34  
35 25 **Google Earth 7.1.** (2017) 6°06'12.46S, 81°53'08.372W to 67°21'20.632S,  
36 26 0°26'24.892E. US Dept of State Geographer Image Landsat / Copernicus, Data SIO,  
37 27 NOAA, U.S. Navy, NGA, GEBCO. Viewed 18/07/2017  
38  
39 28 **Haughton, P.D.W., Barker, S.P. & McCaffrey, W.D.** (2003). "Linked debrites in  
40 29 sand-rich turbidite systems – origin and significance. *Sedimentology*, 50, 459-482.  
41  
42 30 **Haughton, P.D.W., Davis, C., McCaffrey, W.D. & Barker, S.** (2009) Hybrid  
43 31 sediment gravity flow deposits – Classification, origin and significance. *Marine and*  
44 32 *Petroleum Geology*, 26, 1900-1918.  
45  
46 33 **Hempton, M., Marhsall, J., Sadler, S., Hogg, N., Charles, R., & Harvey C.** (2005)  
47 34 Turbidite reservoirs of the Sele Formation, Central North Sea: geological challenges  
48 35 for improving production. In: Dore, A.G. & Vining, B.A., (eds) *Petroleum Geology:*  
49 36 *North-West Europe and Global Perspectives – Proceedings of the 6<sup>th</sup> Petroleum*  
50 37 *Geology Conference*, 449-459.  
51  
52  
53  
54  
55  
56  
57  
58  
59  
60

- 1  
2  
3 1 **Hodgson, D.M.** (2009) Distribution and origin of hybrid beds in sand-rich submarine  
4 2 fans of the Tanqua depocentre, Karoo Basin, South Africa. *Marine and Petroleum*  
5 3 *Geology*, 26, 1940-1957.
- 6  
7 4 **Holmes, N., Atkin, D., Mahdi, S., & Ayress, M.** (2015). Integrated biostratigraphy  
8 5 and chemical stratigraphy in the development of a reservoir-scale stratigraphic  
9 6 framework for the Sea Lion Field area, North Falkland Basin. *Petroleum Geoscience*,  
10 7 21(2-3), 171-182.
- 11  
12 8 **Jungslager, E.H.A.** (1999) Petroleum habits of the Atlantic margin of South Africa.  
13 9 *In: Cameron, N.R., Bate, R.H. & Clurie, V.S. (eds) The Oil and Gas Habitats of the*  
14 10 *South Atlantic. Geological Society, London, Special Publications*, 153, 153-168.
- 15  
16 11 **Kane, I. A., Catterall, V., McCaffrey, W. D., & Martinsen, O. J.** (2010). Submarine  
17 12 channel response to intrabasinal tectonics: The influence of lateral tilt. *AAPG*  
18 13 *bulletin*, 94(2), 189-219.
- 19  
20 14 **Kane, I.A. & Pontén, A.S.M.** (2012) Submarine transitional flow deposits in the  
21 15 Paleogene Gulf of Mexico. Article in *Geology*, Nov 2012 DOI: 10.1130/G33410.1
- 22  
23 16 **Kane, I.A., Pontén, A.S.M. Vangdal, B., Eggenhuisen, J.T., Hodgson, D.M. &**  
24 17 **Spychala, Y.** (2017) The stratigraphic record and processes of turbidity current  
25 18 transformation across deep-marine lobes. *Sedimentology*, 64, 1236-1273.
- 26  
27 19 **Kneller, B.** (2003). The influence of flow parameters on turbidite slope channel  
28 20 architecture. *Marine and Petroleum Geology*, 20(6-8), 901-910.
- 29  
30 21 **Larsen, D. & Smith, G.A.** (1999) Sublacustrine-fan deposition in the Oligocene  
31 22 Creede Formation, Colorado, U.S.A. *Journal of Sedimentary Research*, 69, 675-689.
- 32  
33 23 **Li, Q., Jiang, Z., Liu, K., Zhan, C. & You, X.** (2014) Factors controlling reservoir  
34 24 properties and hydrocarbon accumulation of lacustrine deep-water turbidites in the  
35 25 Huimin Depression, Bohai Bay Basin, East China. *Marine and Petroleum Geology*,  
36 26 57, 327-344.
- 37  
38 27 **Lohr, T. & Underhill, J.R.** (2015) Role of rift transection and punctuated subsidence  
39 28 in the development of the North Falkland Basin. *Petroleum Geoscience*, 21, 85-110.
- 40  
41 29 **Lomas, S.A. & Joseph, P.** (2004) Confined turbidite systems. From: Lomas, S.A. &  
42 30 Joseph P. (eds) (2004) Confined turbidite systems. *Geological Society, London,*  
43 31 *Special Publications*, 222, 1-7.
- 44  
45 32 **Lowe, D. R.** (1979) Sediment Gravity Flows: Their Classification and Some  
46 33 Problems of Application to Natural Flows and Deposits. *SEPM Special Publication*,  
47 34 27, 75-82.
- 48  
49 35 **Lyons, R.P., Scholz, C.A., Buoniconti, M.R. & Martin, M.R.** (2011) Late  
50 36 Quaternary stratigraphic analysis of the Lake Malawi Rift, East Africa: An integration  
51 37 of drill-core and seismic-reflection data. *Journal of Palaeogeography,*  
52 38 *Palaeoclimatology, Palaeoecology*, 203, 20-72.
- 53  
54  
55  
56  
57  
58  
59  
60

- 1 **MacAulay F.** (2015) Sea Lion Field discovery and appraisal: a turning point for the  
2 North Falkland Basin. *Petroleum Geoscience*, 21, 111-124.
- 3 **MacDonald, D., Gomez-Perez, I., Franzese, J., Spalletti, L., Lawver, L.,**  
4 **Gahagan, L., Dalziel, I., Thomas, C., Trewin, N., Hole, M. & Paton, M.** (2003)  
5 Mesozoic break-up of SW Gondwana: implications for regional hydrocarbon potential  
6 of the southern South Atlantic. *Marine and Petroleum Geology*, 20, 287-308.
- 7 **Mayall, M., Jones, E. & Casey, M.** (2006) Turbidite channel reservoirs – Key  
8 elements in facies prediction and effective development. *Marine and Petroleum*  
9 *Geology*, 23, 821-841.
- 10 **Mayall, M., Lonergan, L., Bowman, A., James, S., Mills, K., Primmer, T., Pope,**  
11 **D., Rogers, L. & Skeene, R.** (2010) The response of turbidite slope channel to  
12 growth-induced seabed topography. *AAPG Bulletin*, 94, 7, 1011-1030.
- 13 **Moernaut, J., Van Daele, M., Heirman, K., Fontijn, K., Strasser, M., Pino, M.,**  
14 **Urrutia, R. & M. De Batist,** (2014). Lacustrine turbidites as a tool for quative  
15 earthquake reconstruction: New evidence for variable rupture mode in south central  
16 Chile. *Journal of Geophysical Research: Solid Earth*, 119, 1607-1633.
- 17 **Mutti, E. & Nilsen, T.** (1981) Significance of intraformational rip-up clasts in deep-  
18 sea fan deposits. *Int. Assoc. Sedimentol. 2nd Eur. Regional Mtg. Abstr., Bologna,*  
19 pp. 117-119.
- 20 **Mutti, E., & Normark, W. R.** (1987). Comparing examples of modern and ancient  
21 turbidite systems: problems and concepts. In *Marine clastic sedimentology* (pp. 1-  
22 38). Springer, Dordrecht.
- 23 **Mutti, E.** (1992) (ed) *Turbidite Sandstones*. AGIP Istituto di geologia, Università di  
24 Parma, Italy, 275-276.
- 25 **Mutti, E., Davoli, G., Mora, S. & Papani, L.** (1994) Internal Stacking Patterns of  
26 Ancient Turbidite Systems from Collisional Basins. In: *Submarine fans and turbidite*  
27 *systems: Gulf Coast Section SEPM Proceedings, 15th Annual Research*  
28 *Conference*, 15, 257-268.
- 29 **Mutti, E., Tinterri, R., Benevelli, G., Biase, D. & Cavanna, G.** (2003) Deltaic, mixed  
30 and turbidite sedimentation of ancient foreland basins. *Marine and Petroleum*  
31 *Geology*, 20, 733-755.
- 32 **Nelson, C.H., Karabanov, E.B., Colman, S.M. & Escutia, C.** (1999) Tectonic and  
33 sediment supply control of deep rift lake turbidite system, Lake Baikal, Russia.  
34 *Geology*, 27, 163-166.
- 35 **Porten, K.W., Kane, I.A., Warchol, M.J. & Southern, S.J.** (2016) A  
36 sedimentological process-based approach to depositional reservoir quality of deep-  
37 marine sandstones: an example from the Springar Formation, north-western Vøring  
38 Basin, Norwegian Sea, *Journal of Sedimentary Research*, 86, 11, 1269-1286.

- 1  
2  
3 1 **Posamentier, H.W. & Kolla, V.** (2003) Seismic geomorphology and stratigraphy of  
4 2 depositional elements in deep-water settings. *Journal of Sedimentary Research*, 73,  
5 3 3, 367-388.  
6  
7 4 **Postma, G., Nemec, W. & Kleinspehn, K.L.** (1988) Large floating clasts in  
8 5 turbidites: a mechanism for their emplacement. *Sedimentary Geology*, 58, 47-61.  
9  
10 6 **Prelat, A., Flint, S. & Hodgson, D.M.** (2009) Evolution, architecture and hierarchy of  
11 7 distributory deep-water deposits: a high-resolution outcrop investigation from the  
12 8 Permian Karoo Basin, South Africa. *Sedimentology*, 56, 2132-2154.  
13  
14 9 **Prather, B.E., Booth, J.R., Steffens, G.S. & Craig, P.A.** (1998a) Classification,  
15 10 Lithologic Calibration, and Stratigraphic Succession of Seismic Facies of Intraslope  
16 11 Basins, Deep-Water Gulf of Mexico. *AAPG Bulletin*, 82, 5A, 701-728.  
17  
18 12 **Richards, M., Bowman, M. & Reading, H.** (1998) Submarine-fan systems I:  
19 13 characterisation and stratigraphic prediction. *Marine and Petroleum Geology*, 15,  
20 14 689-717.  
21  
22 15 **Richards, M. & Bowman, M.** (1998) Submarine fans and related depositional  
23 16 systems II: variability in reservoir architecture and wireline log character. *Marine and*  
24 17 *Petroleum Geology*, 15, 821-839.  
25  
26 18 **Richards, P.C., Gatliff, R.W., Quinn, M.F. & Fannin, N.G.T.** (1996a) Petroleum  
27 19 Potential of the Falkland Islands Offshore Area. *Journal of Petroleum Geology*, 19,  
28 20 161-182.  
29  
30 21 **Richards, P.C., Gatliff, R.W., Quinn, M.F., Williamson, J.P. & Fannin N.G.T.**  
31 22 (1996b) The geological evolution of the Falkland Islands continental shelf. From:  
32 23 Storey, B.C., King, E.C., & Livermore, R.A., (eds), 1996 Weddel Sea Tectonics and  
33 24 Gondwana Break-up, *Geological Society Special Publication*, 108, 105-128.  
34  
35 25 **Richards, P.C. & Fannin N.G.T.** (1997) Geology of the North Falkland Basin.  
36 26 *Journal of Petroleum Geology*, 20, 165-183.  
37  
38 27 **Richards, P.C. & Hillier, B.V.** (2000a) Post-drilling Analysis of the North Falkland  
39 28 Basin – Part 1: Tectono-Stratigraphic Framework. *Journal of Petroleum Geology*, 23,  
40 29 253-272.  
41  
42 30 **Richards, P.C. & Hillier B.V.** (2000b) Post-drilling Analysis of the North Falkland  
43 31 Basin – Part 2: The Petroleum System and Future Prospects. *Journal of Petroleum*  
44 32 *Geology*, 23, 273-292.  
45  
46 33 **Richards, P.C., Duncan, I., Phipps, c., Pickering, G., Grzywacz, J., Hault, R. &**  
47 34 **Meritt, J.** (2006) Exploring for Fan Delta Sandstones in the Offshore Falkland  
48 35 Islands. *Journal of Petroleum Geology*, 29, 199-214.  
49  
50 36 **Romans, B.W., Hubbard, S.M. & Graham, S.A.** (2009) Stratigraphic evolution of an  
51 37 outcropping continental slope system, Tres Pasos Formation at Cerro Divisadero,  
52 38 Chile. *Sedimentology*, 56, 737-764.  
53  
54  
55  
56  
57  
58  
59  
60

- 1  
2  
3 1 **Ronghe, S. & Surarat, K.** (2002) Acoustic impedance interpretation for sand  
4 2 distribution adjacent to a rift boundary fault, Suphan Buri basin, Thailand. *AAPG*  
5 3 *Bulletin*, 86, 10, 1753-177.  
6  
7 4 **Saez, A. & Cabrera, L.** (2002) Sedimentological and palaeohydrological responses to  
8 5 tectonics and climate in a small, closed, lacustrine system: Oligocene As Pontes  
9 6 Basin (Spain). *Sedimentology*, 49, 1073-1094.  
10  
11 7 **Saller, A., Werner, K., Sugiaman, F., Cebastiant, A., May, R., Glen, D. & Barker,**  
12 8 **C.** (2008) Characteristics of Pleistocene deep-water fan lobes and their application to  
13 9 an upper Miocene reservoir model, offshore East Kalimantan, Indonesia. *AAPG*  
14 10 *Bulletin*, Vol. 92, No. 7, pp. 919-949.  
15  
16 11 **Scholz C.A., Rosendahl B.R. & Scott, D.L.** (1990) Development of coarse-grained  
17 12 facies in lacustrine rift basins: Examples from East Africa, *Geology*, 18, 140-144.  
18  
19 13 **Shanmugam, G., Shrivastava, S.K. & Bhagaban, D.** (2009) Sandy debrites and  
20 14 tidalites of Pliocene reservoir sand in upper-slope canyon environments, offshore  
21 15 Krishna-Godavari Basin (India): Implications. *Journal of Sedimentary Research*, 79,  
22 16 736-756.  
23  
24 17 **Shanmugam, G. & Moiola, R.J.** (1988) Submarine Fans: Characteristics, Models,  
25 18 Classification, and Reservoir Potential. *Earth Science Reviews*, 24, 383-428.  
26  
27 19 **Simm, R. & Bacon, M.** (2014) *Seismic Amplitude: An Interpreter's Handbook*.  
28 20 Cambridge University Press, ISBN 978-1-107-01150-2.  
29  
30 21 **Smith, R.D.A.** (1995) Reservoir architecture of syn-rift lacustrine turbidite systems,  
31 22 early Cretaceous, offshore South Gabon. *Geological Society, London, Special*  
32 23 *Publications*, 80, 197-210.  
33  
34 24 **Southern, S. J., Mountney, N. P., & Pringle, J. K.** (2014). The Carboniferous  
35 25 Southern Pennine Basin, UK. *Geology Today*, 30(2), 71-78.  
36  
37 26 **Southern S.J., Patacci, M., Felletti, F. & McCaffrey W.D.** (2015) Influence of flow  
38 27 containment and substrate entrainment upon sandy hybrid event beds containing co-  
39 28 genetic mud-clast-rich division. *Sedimentary Geology*, 321, 105-122.  
40  
41 29 **Southern, S.J., Kane, I.A., Warchol, M.J., Porten, K.W. & McCaffrey, W.D.** (2017)  
42 30 Hybrid event beds dominated by transitional-flow facies: character, distribution and  
43 31 significance in the Maastrichtian Springar Formation, north-west Voring Basin,  
44 32 Norwegian Sea. *Sedimentology*, 64, 747-776.  
45  
46 33 **Spears, D.A.** (2012) The origin of tonsteins, an overview, and links with seatearths,  
47 34 fireclays and fragmental clay rocks. *International Journal of Coal Geology*, 94, 22-31.  
48  
49 35 **Stevenson, C.J., Jackson, C.A.L., Hodgson, D.M., Hubbard, S.M. &**  
50 36 **Eggenhuisen, J.T.** (2015) Deep-Water Sediment Bypass. *Journal of Sedimentary*  
51 37 *Research*, 85, 1058-1081.  
52  
53 38 **Stow, D. A., & Mayall, M.** (2000). Deep-water sedimentary systems: new models for  
54 39 the 21st century. *Marine and Petroleum Geology*, 17(2), 125-135.  
55  
56  
57  
58  
59  
60

- 1  
2  
3 1 **Straub, K. M., & Pyles, D. R.** (2012). Quantifying the hierarchical organization of  
4 2 compensation in submarine fans using surface statistics. *Journal of Sedimentary*  
5 3 *Research*, 82(11), 889-898.  
6  
7 4 **Talling, P.J.** (2013) Hybrid submarine flows comprising turbidity current and  
8 5 cohesive debris flow: Deposits, theoretical and experimental analyses, and general  
9 6 models. *Geosphere*, 9, 3, 460-488.  
10  
11 7 **Tan, M., Zhu, X., Geng, M., Zhu, S., & Liu, W.** (2017). The occurrence and  
12 8 transformation of lacustrine sediment gravity flow related to depositional variation  
13 9 and paleoclimate in the Lower Cretaceous Prosopis Formation of the Bongor Basin,  
14 10 Chad. *Journal of African Earth Sciences*, 134, 134-148.  
15  
16 11 **Terlaky, V. & Arnott, R.W.C.A.** (2014) Matrix-rich and associated matrix-poor  
17 12 sandstones: Avulsion splays in slope and basin-floor strata. *Sedimentology*, 61,  
18 13 1175-1197.  
19  
20 14 **Williams, L.S.** (2015) Sedimentology of the Lower Cretaceous reservoirs of the Sea  
21 15 Lion Field, North Falkland Basin. *Petroleum Geoscience*, 21, 183-198.  
22  
23 16 **Williams, L.S. & Newbould, R.** (2015). Introduction to the North Falkland Basin  
24 17 revisited: exploration and appraisal of the Sea Lion Field. *Petroleum Geoscience*, 21,  
25 18 83-84.  
26  
27 19 **Winker, C. D.** (1996). High-resolution seismic stratigraphy of a late Pleistocene  
28 20 submarine fan ponded by salt-withdrawal mini-basins on the Gulf of Mexico  
29 21 continental slope. In *Offshore Technology Conference*. Offshore Technology  
30 22 Conference.  
31  
32 23 **Zhang, S.** (2004) The application of an integrated approach in exploration of  
33 24 lacustrine turbidites in Kiyang Sub-basin, Bohai Bay Basin, China. *Journal of*  
34 25 *Petroleum Science and Engineering*, 41, 67-77.  
35  
36 26 **Zhi-qiang, F., Shun, Z., Cross, T.A., Zi-hui, F., Xi-nong, X., Bo, Z., Xiu-li, F. &**  
37 27 **Cheng-shan, W.** (2010) Lacustrine turbidite channels and fans in the Mesozoic  
38 28 Songliao Basin, China. *Basin Research*, 22, 96-107.  
39  
40  
41  
42 29  
43  
44  
45  
46  
47  
48  
49  
50  
51  
52  
53  
54  
55  
56  
57  
58  
59  
60

1  
2  
3 **1 Table Captions**

4  
5  
6 2 Table 1). - Description and core photographs of sedimentary facies from the Sea  
7  
8 3 Lion Fan

9  
10  
11 4 Table 1 cntd.) - Description and core photographs of sedimentary facies from the  
12  
13 5 Sea Lion Fan

14  
15  
16 **6 Figure Captions**

17  
18  
19 7 **Figure 1.** Map showing the location of the Falkland Islands located around 300 km to  
20  
21 8 the southeast of South America (inset). The Falkland Islands are surrounded by  
22  
23 9 several Mesozoic offshore basins including the NFB containing the Sea Lion Fan,  
24  
25 10 which was deposited along one of the major north-south trending basin-bounding  
26  
27 11 faults.

28  
29  
30  
31 12 **Figure 2.** Line A-A' - Interpreted east-west orientated seismic line through the Sea  
32  
33 13 Lion Fan of the NFB half-graben. The 14/10-2 Sea Lion discovery well encountered  
34  
35 14 oil along the eastern flank of the NFB, in the LC3 tectono-stratigraphic unit, within the  
36  
37 15 early post-rift basin fill.

38  
39  
40 16 **Figure 3.** Stratigraphic column, displaying lithostratigraphical nomenclature for the  
41  
42 17 NFB, modified after Richards and Hillier (2000a) and MacAulay (2015).

43  
44  
45 18 **Figure 4.** A series of full-stack, zero-phase, European polarity seismic and  
46  
47 19 geoseismic sections, fan polygons and map illustrating the overlapping nature of the  
48  
49 20 Sea Lion North Fan, Otter Fan and the Sea Lion Fan with composite lobes. **A.**  
50  
51 21 Section A-A' illustrates the proximal setting, and shows the distribution of the  
52  
53 22 overlapping tabular sands. **B.** Section B-B' illustrates the geometries of medial fan,  
54  
55 23 characterised by overstepping, compensational stacking patterns. **C.** Section C-C'

1 illustrates the distal overstepping geometries of the Sea Lion Fan lobes, more  
2 particularly how the SL15 lobe overlaps the SL20 lobe in the distal locations.

3 **Figure 5.** North-south-east orientated, correlated wireline logs (gamma-ray) hung on  
4 2523.60 m (MD SSL). Moving from north-to-south, this correlation panel displays the  
5 SL15, SL20, SL10 lobes and the Otter Fan, which all rest on a lowstand surface,  
6 representing the base of LC3 (BGS seismic pick “event 5.3”). Correlations are based  
7 on seismic interpretation, in particular stacking geometries (indications for  
8 overlapping) and the determination of relative stacking patterns. The SL20 lobe  
9 represents the oldest deposits, which are overlain by the SL15 lobe and the SL10  
10 lobe.

11 **Figure 6.** Idealised facies associations and bed types from cored sections of the Sea  
12 Lion Fan. The facies descriptions for the facies codes, referred to in this diagram, are  
13 contained within Table 1. **i.)** Lobe Axis facies association, **ii.)** Lobe Fringe facies  
14 association. **iii.)** Lobe Distal Fringe facies association. **iv.)** Hemi-Limnic Mudstones  
15 facies association **v.)** Deformed Sandstones and Mudstones facies association **vi.)**  
16 Hybrid Event Bed (bed type).

17 **Figure 7.** Interpreted seismic amplitude extraction maps of the Sea Lion North Fan,  
18 the Otter Fan and the Sea Lion Fan, displaying the Sea Lion Fan’s component lobes:  
19 SL 10, SL 15, SL 20. Seismic amplitude extractions have been calculated from +/- 10  
20 ms above a single, tabular seismic reflector. **A.** Composite map of three easterly  
21 derived fans, demonstrating the Sea Lion North Fan, the Sea Lion Fan’s SL 10, SL  
22 15, SL 20 lobes and the Otter Fan. The Sea Lion Fan comprises no less than three  
23 separate lobes, emanating from the same feeder position, located along the eastern  
24 flank of the NFB. **B.** The SL 10 lobe of the Sea Lion Fan. **C.** The SL 15 lobe of the

1 Sea Lion Fan. The distribution of the Sea Lion North Fan is marked by the dashed  
2 line, illustrating evidence for deflection of flow by pre-existing topography, formed by  
3 deposits of the older Sea Lion North Fan. **D.** The SL 20 lobe of the Sea Lion Fan.

4 **Figure 8.** Representative core photography from the Sea Lion Fan illustrating the  
5 range and type of sedimentary features. **A.** Core from the SL10 lobe . i. *fss*, *frxls* and  
6 *fplm* observed in well 14/10-5. ii. *fss* iii. *fss*, *fpls* and *fplm*. **B.** Core from the SL20  
7 lobe. i. *fss* ii. *fpls* and *fss* iii. *fss* and *fplm*. **C.** Core from the SL15 lobe. i. dewatered  
8 *fss* ii. *fss* iii. *fss*. **D.** Core from the Sea Lion North Fan i. dewatered *fss* ii. dewatered  
9 *fss* and *fpls* iii. dewatered *fss*, *fplm* and *frxls*.

10 **Figure 9.** Examples of hybrid event beds from SL15, observed in wells 14/10-6  
11 (2456.20 m) and 14/10-7 (2469.50 m). **A.** A hybrid event bed in 14/10-6, comprising  
12 the *fab1-3* facies succession and underlying structureless sandstone. **B.** Two  
13 stacked hybrid event beds in 14/10-7, with the upper-most facies, *fab3*, absent. In  
14 both examples, *fab2* contains a concentration of mudclasts. Instances of facies  
15 *fab3*, contain a concentration of carbonaceous clasts and smaller carbonaceous  
16 flecks in the matrices.

17 **Figure 10.** Examples of core photography from the Sea Lion Fan, displaying  
18 deformed sandstones and mudstones. **A.** A highly deformed, rotated, laminated unit  
19 that exists below a thick sandstone succession, interpreted as the flanks of a mud-  
20 volcano, which formed in response to dewatering of the lower beds by the imposing  
21 over-burden of the sandstones. **B.** Soft-sediment deformation, with tearing and  
22 stretching of more competent, yet ductile mudstone units by the injection of coarser-  
23 grained, fluidised material. This style of mudstone deformation suggests partial  
24 lithification of the mudstones prior to disruption.

1 **Figure 11.** Correlated sedimentary core logs through the Sea Lion Fan (see Figure  
2 7a. for the correlation map). The sedimentary logs have been colour-coded based on  
3 identified facies associations, which are illustrated in the facies key. Note the location  
4 of hybrid event beds in the SL15 lobe. Gaps in the logs represent preserved  
5 samples, which were unavailable for logging.

6 **Figure 12.** Three dimensional seismic amplitude surface showing: points of  
7 sediment entry into the basin; the location of the Sea Lion North and Sea Lion fans;  
8 and interpreted depositional facies for the Sea Lion Fan. The seismic surface  
9 comprises a 50 ms window of averaged seismic amplitudes from above the  
10 Valanginian-aged unconformity surface on to which the fans were deposited. The  
11 Sea Lion Fan was sourced from a feeder system located to the south of that which  
12 fed the Sea Lion North Fan. Distal delta-toe architectures, sourced from the north,  
13 inter-digitate with deposits of the Sea Lion Fan.

14 **Figure 13.** Schematic depositional model for the Sea Lion Fan, and more generally a  
15 model for deep-lacustrine turbidite deposition. Lobe axis deposits are located in the  
16 more axial positions and are represented by thick successions of stacked,  
17 amalgamated, high-density turbidites that comprise structureless sandstone. The  
18 lobe axis deposits are focussed along sinuous corridors, controlled by partial  
19 confinement. The lobe fringe deposits comprise high-density turbidites that are  
20 typically thinner and less-amalgamated with greater preservation of fine grained,  
21 parallel to current ripple laminated bed tops along with the presence of more regular,  
22 thicker-bedded hemi-limnic mudstones. Hybrid event beds are observed in lobe  
23 fringe depositional locations, associated with the isolated occurrences of  
24 structureless sandstone. Lobe distal fringe deposits are dominated by low-density

1 turbidites that largely comprise parallel-laminated to ripple laminated sandstones and  
2 preservation of pervasive hemi-limnic mudstones.

3 **Figure 14.** Schematic depositional environment for the NFB, during the Valanginian  
4 low-stand of the lake. A major axial delta prograded into the basin from the north,  
5 contemporaneously with the inclusion of the turbidite fans. These fans entered the  
6 basin from the eastern flank, forming sand-rich, slope apron features, draping the  
7 eastern basin slopes. Presence of detrital glauconite in these deposits suggests  
8 some element of pre-sorting in the shallow water environment, perhaps from a  
9 shelfal bar or fan delta. There is further evidence for Sea Lion-style fans, both  
10 geographically and stratigraphically throughout the NFB, indicating the potential for  
11 high sedimentation rates in the basin throughout the early Cretaceous.

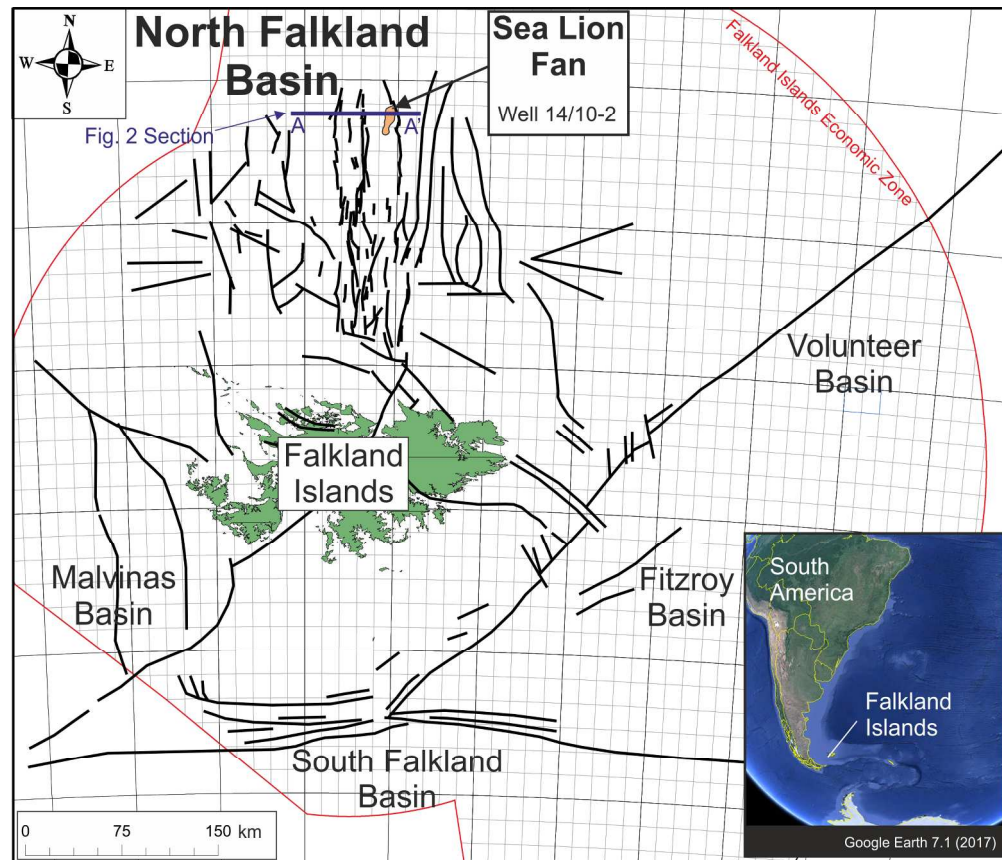


Figure 1. Map showing the location of the Falkland Islands located around 300 km to the southeast of South America (inset). The Falkland Islands are surrounded by several Mesozoic offshore basins including the NFB containing the Sea Lion Fan, which was deposited along one of the major north-south trending basin-bounding faults.

200x171mm (300 x 300 DPI)

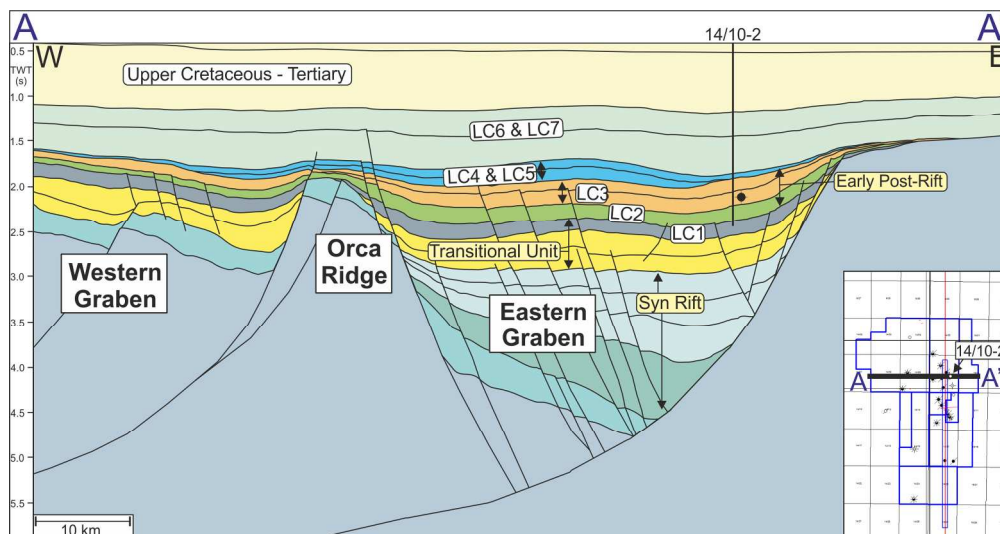


Figure 2. Line A-A' - Interpreted east-west orientated seismic line through the Sea Lion Fan of the NFB half-graben. The 14/10-2 Sea Lion discovery well encountered oil along the eastern flank of the NFB, in the LC3 tectono-stratigraphic unit, within the early post-rift basin fill.

193x101mm (300 x 300 DPI)

Period	Epoch	Age	Richards and Hillier, 2000a Tectono-Stratigraphy		MacAulay, 2015 Stratigraphy	Eastern Margin Fans	
						N	S
Cretaceous	Lower	Aptian - Albian	Middle Post -Rift	LC7	D4 - D9		
				LC6			
		Valanginian - early Aptian	Early Post-Rift	LC4 and LC5	E1-E3		
				LC3	F1		
					F2		
				LC2	F3		
		LC1					
				Transitional Unit			
?Jurassic	?Upper	Turonian - Berriasian	Late Syn-Rift	"J2"	G1-2		

Figure 3. Stratigraphic column, displaying lithostratigraphical nomenclature for the NFB, modified after Richards and Hillier (2000a) and MacAulay (2015).

291x177mm (300 x 300 DPI)

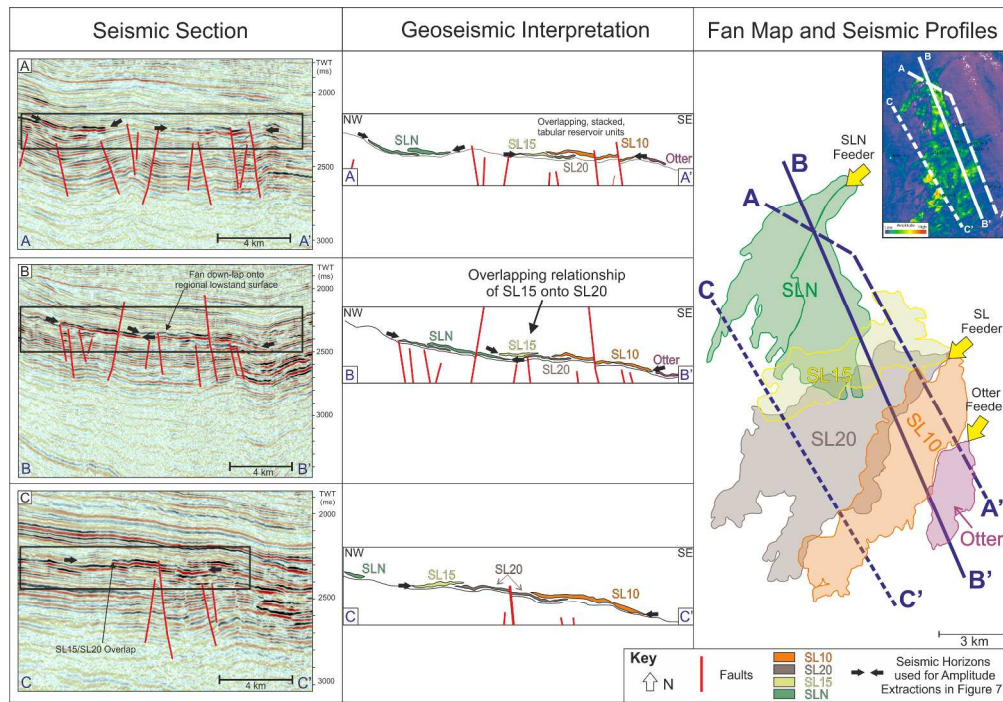


Figure 4. A series of full-stack, zero-phase, European polarity seismic and geoseismic sections, fan polygons and map illustrating the overlapping nature of the Sea Lion North Fan, Otter Fan and the Sea Lion Fan with composite lobes. A. Section A-A' illustrates the proximal setting, and shows the distribution of the overlapping tabular sands. B. Section B-B' illustrates the geometries of medial fan, characterised by overstepping, compensational stacking patterns. C. Section C-C' illustrates the distal overstepping geometries of the Sea Lion Fan lobes, more particularly how the SL15 lobe overlaps the SL20 lobe in the distal locations.

290x201mm (300 x 300 DPI)

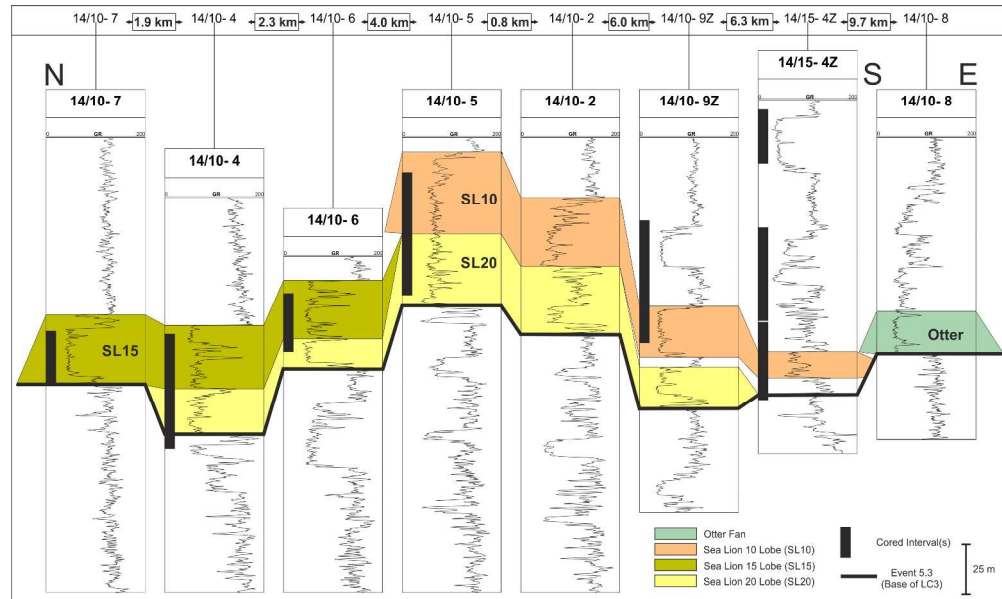


Figure 5. North-south-east orientated, correlated wireline logs (gamma-ray) hung on 2523.60 m (MD SSL). Moving from north-to-south, this correlation panel displays the SL15, SL20, SL10 lobes and the Otter Fan, which all rest on a lowstand surface, representing the base of LC3 (BGS seismic pick "event 5.3").

Correlations are based on seismic interpretation, in particular stacking geometries (indications for overlapping) and the determination of relative stacking patterns. The SL20 lobe represents the oldest deposits, which are overlain by the SL15 lobe and the SL10 lobe.

285x169mm (300 x 300 DPI)

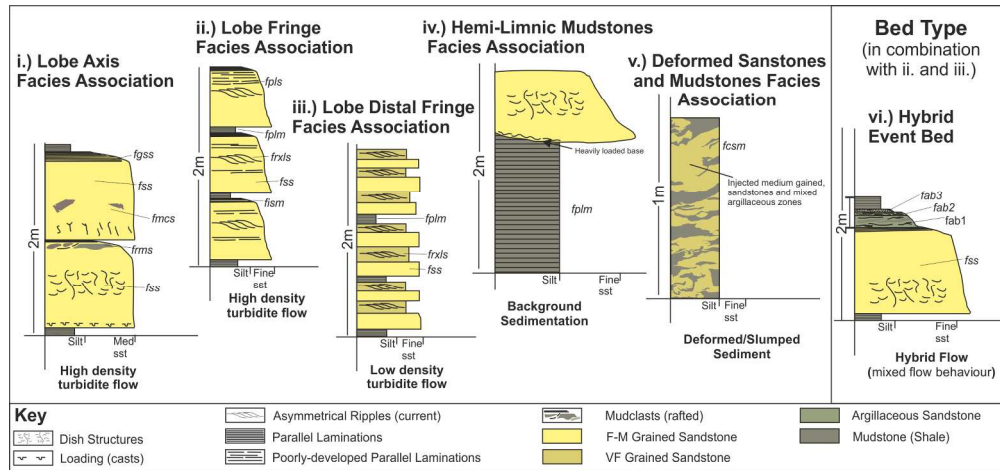


Figure 6. Idealised facies associations and bed types from cored sections of the Sea Lion Fan. The facies descriptions for the facies codes, referred to in this diagram, are contained within Table 1. i.) Lobe Axis facies association, ii.) Lobe Fringe facies association. iii.) Lobe Distal Fringe facies association. iv.) Hemi-Limnic Mudstones facies association v.) Deformed Sandstones and Mudstones facies association vi.) Hybrid Event Bed (bed type).

202x94mm (300 x 300 DPI)

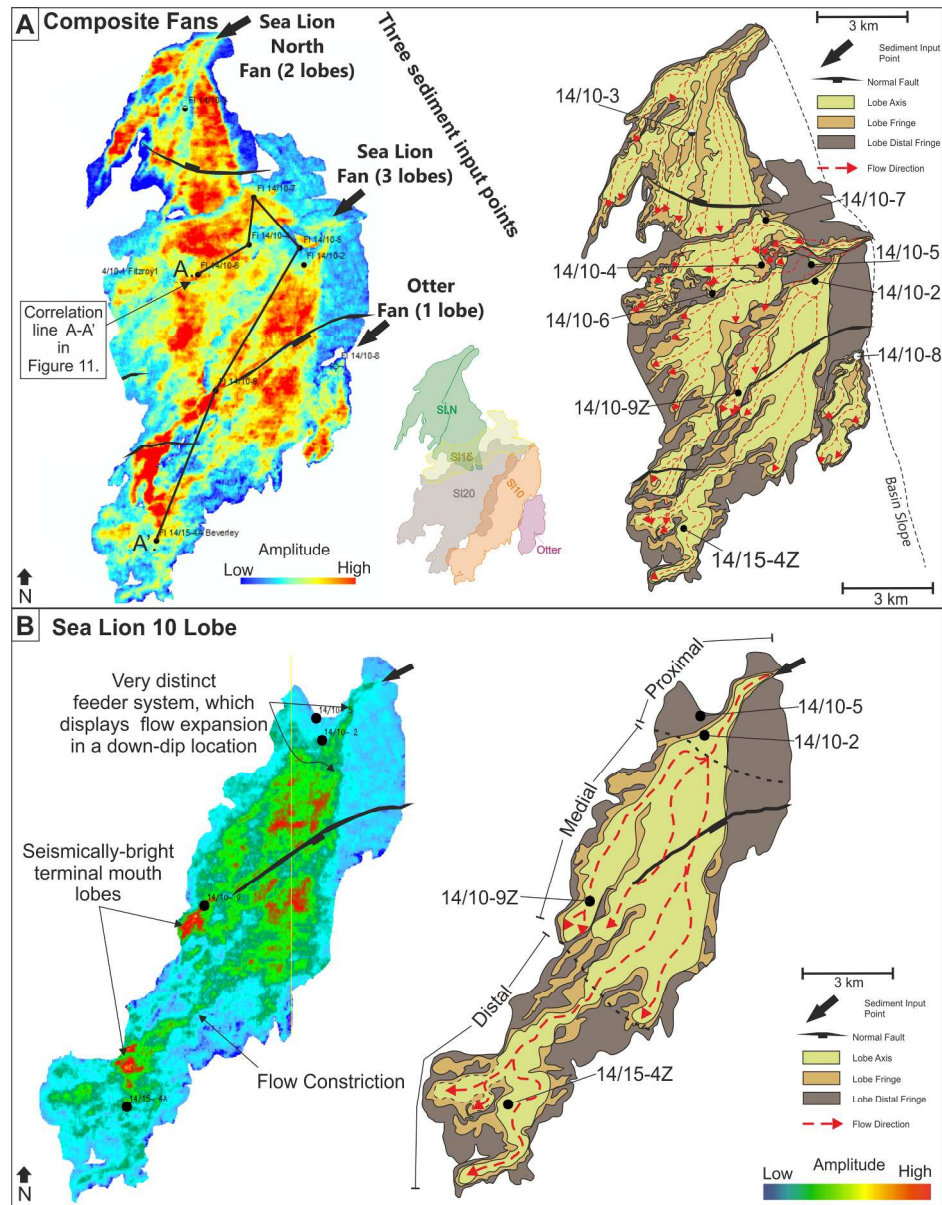
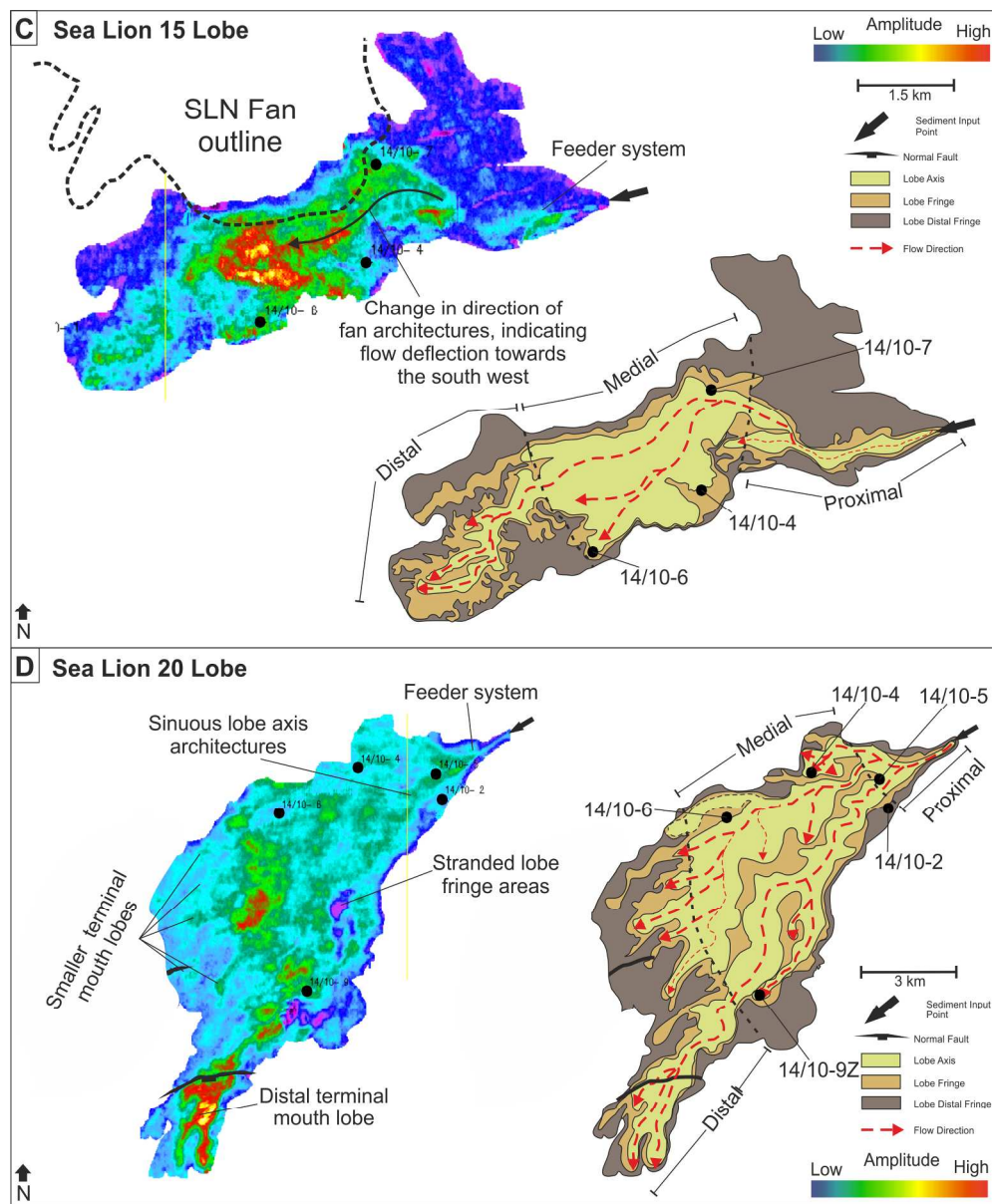


Figure 7. Interpreted seismic amplitude extraction maps of the Sea Lion North Fan, the Otter Fan and the Sea Lion Fan, displaying the Sea Lion Fan's component lobes: SL 10, SL 15, SL 20. Seismic amplitude extractions have been calculated from  $\pm 10$  ms above a single, tabular seismic reflector. A. Composite map of three easterly derived fans, demonstrating the Sea Lion North Fan, the Sea Lion Fan's SL 10, SL 15, SL 20 lobes and the Otter Fan. The Sea Lion Fan comprises no less than three separate lobes, emanating from the same feeder position, located along the eastern flank of the NFB. B. The SL 10 lobe of the Sea Lion Fan.

204x263mm (300 x 300 DPI)



45  
46  
47  
48  
49

Figure 7. (cntd) C. The SL 15 lobe of the Sea Lion Fan. The distribution of the Sea Lion North Fan is marked by the dashed line, illustrating evidence for deflection of flow by pre-existing topography, formed by deposits of the older Sea Lion North Fan. D. The SL 20 lobe of the Sea Lion Fan.

206x249mm (300 x 300 DPI)

50  
51  
52  
53  
54  
55  
56  
57  
58  
59  
60

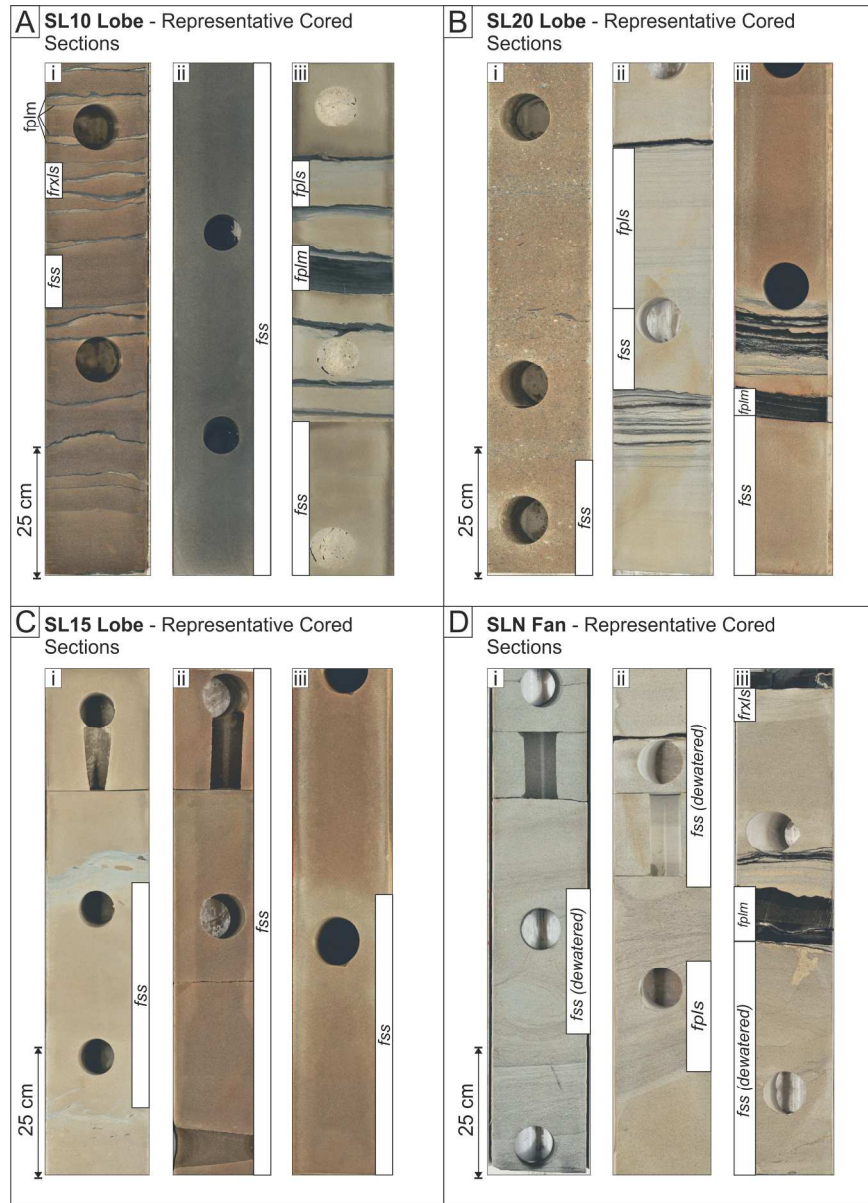


Figure 8. Representative core photography from the Sea Lion Fan illustrating the range and type of sedimentary features. A. Core from the SL10 lobe . i. fss, frxls and fplm observed in well 14/10-5. ii. fss iii. fss, fpls and fplm. B. Core from the SL20 lobe. i. fss ii. fpls and fss iii. fss and fplm. C. Core from the SL15 lobe. i. dewatered fss ii. fss iii. fss. D. Core from the Sea Lion North Fan i. dewatered fss ii. dewatered fss and fpls iii. dewatered fss, fplm and frxls.

186x258mm (300 x 300 DPI)

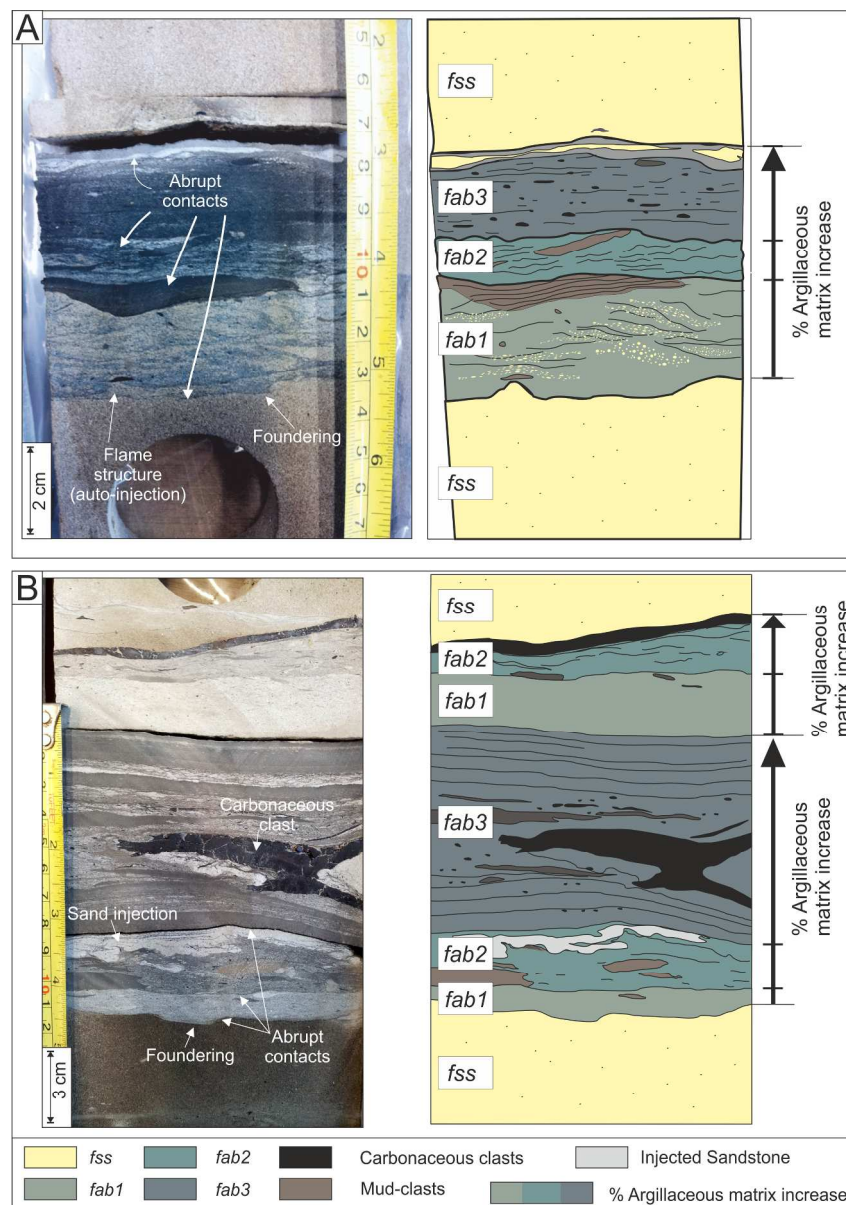


Figure 9. Examples of hybrid event beds from SL15, observed in wells 14/10-6 (2456.20 m) and 14/10-7 (2469.50 m). A. A hybrid event bed in 14/10-6, comprising the fab1-3 facies succession and underlying structureless sandstone. B. Two stacked hybrid event beds in 14/10-7, with the upper-most facies, fab3, absent. In both examples, fab2 contains a concentration of mudclasts. Instances of facies fab3, contain a concentration of carbonaceous clasts and smaller carbonaceous flecks in the matrices.

203x290mm (300 x 300 DPI)



Figure 10. Examples of core photography from the Sea Lion Fan, displaying deformed sandstones and mudstones. A. A highly deformed, rotated, laminated unit that exists below a thick sandstone succession, interpreted as the flanks of a mud-volcano, which formed in response to de-watering of the lower beds by the imposing over-burden of the sandstones. B. Soft-sediment deformation, with tearing and stretching of more competent, yet ductile mudstone units by the injection of coarser-grained, fluidised material. This style of mudstone deformation suggests partial lithification of the mudstones prior to disruption.

190x205mm (300 x 300 DPI)

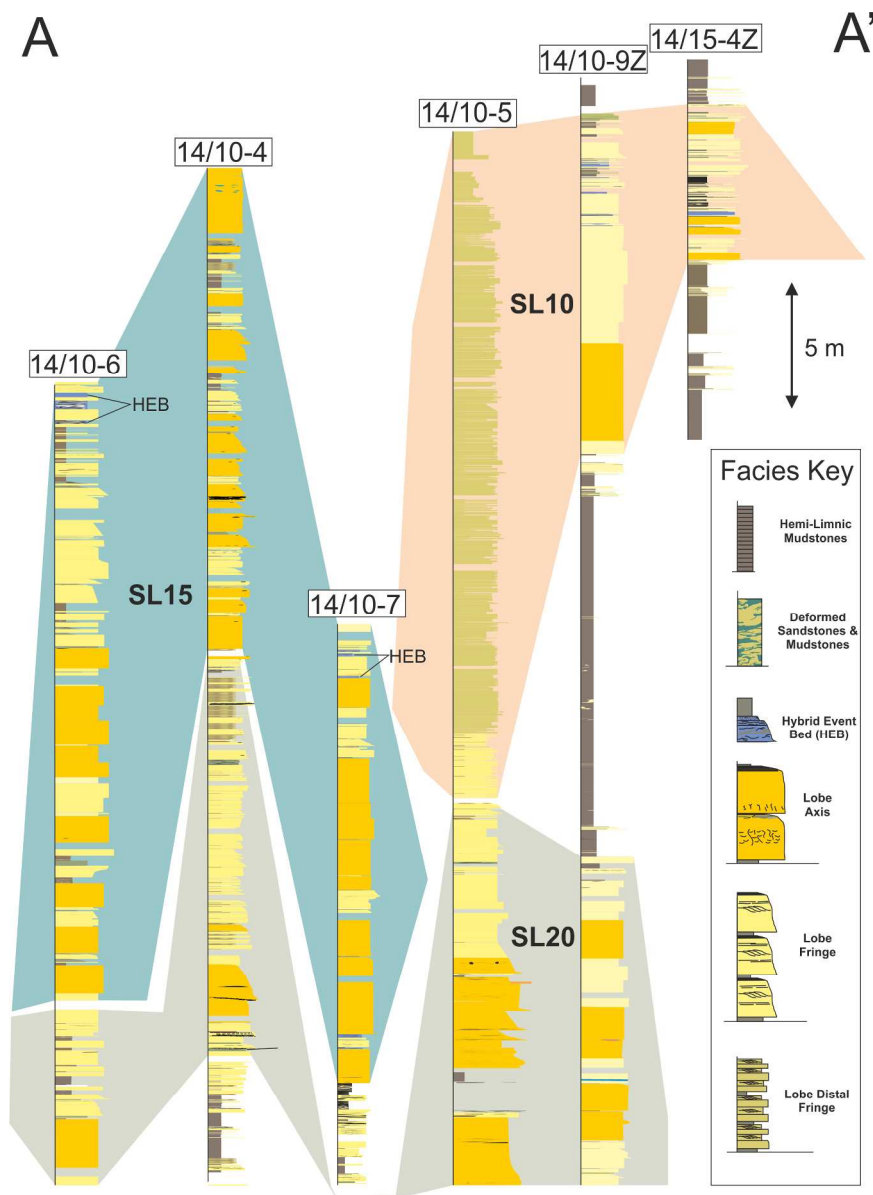


Figure 11. Correlated sedimentary core logs through the Sea Lion Fan (see Figure 7a. for the correlation map). The sedimentary logs have been colour-coded based on identified facies associations, which are illustrated in the facies key. Note the location of hybrid event beds in the SL15 lobe. Gaps in the logs represent preserved samples, which were unavailable for logging.

203x282mm (300 x 300 DPI)

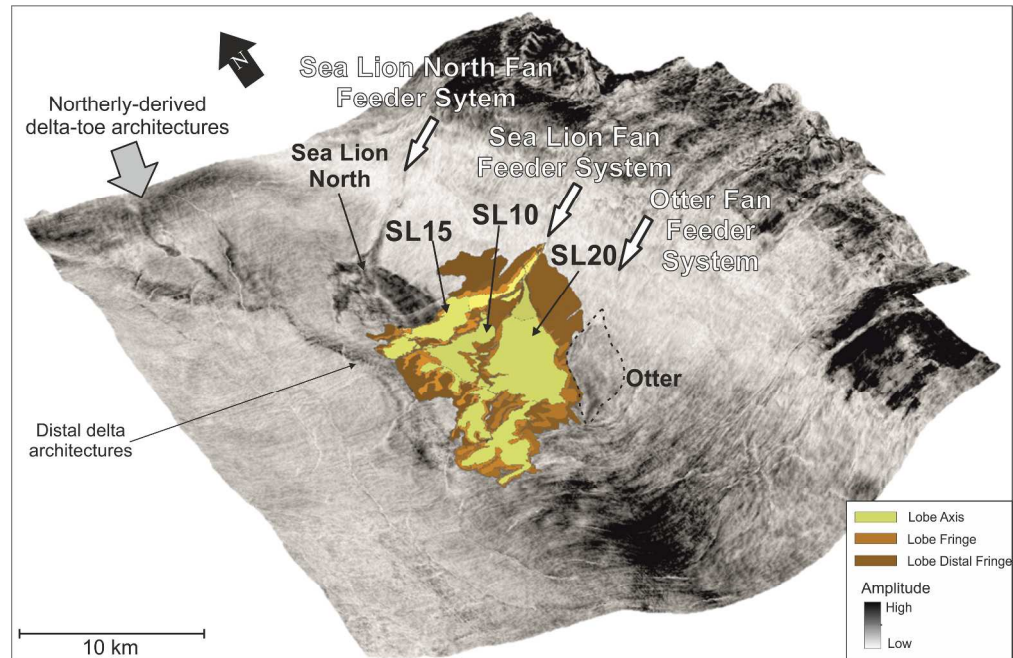
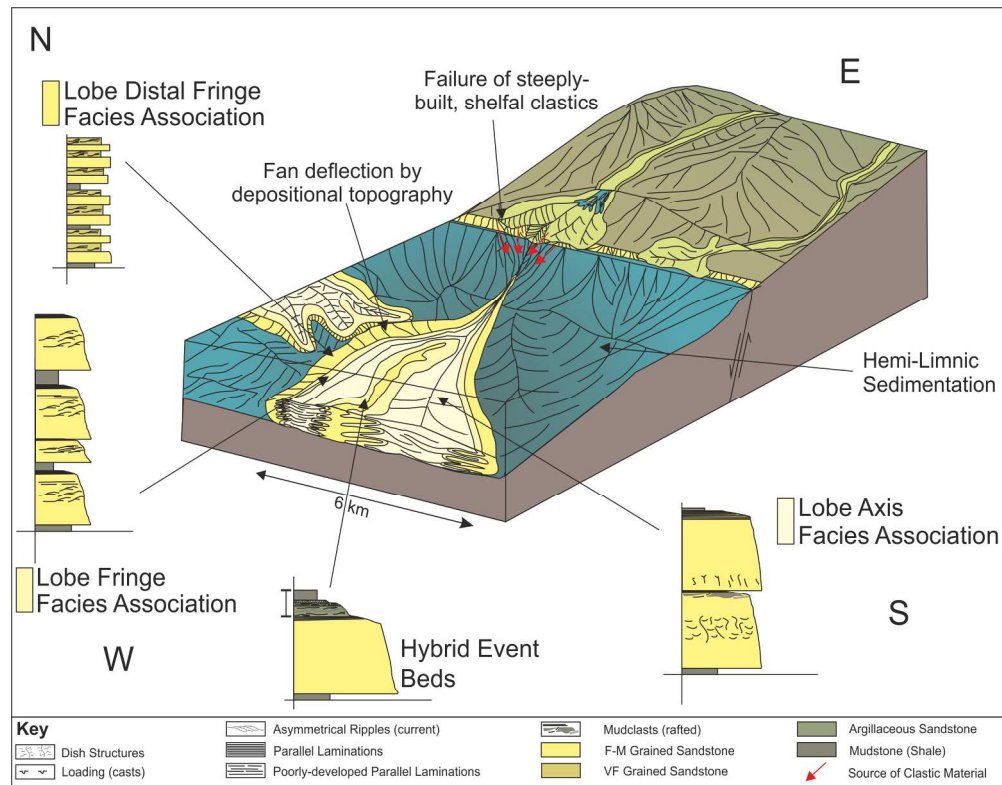


Figure 12. Three dimensional seismic amplitude surface showing: points of sediment entry into the basin; the location of the Sea Lion North and Sea Lion fans; and interpreted depositional facies for the Sea Lion Fan. The seismic surface comprises a 50 ms window of averaged seismic amplitudes from above the Valanginian-aged unconformity surface on to which the fans were deposited. The Sea Lion Fan was sourced from a feeder system located to the south of that which fed the Sea Lion North Fan. Distal delta-toe architectures, sourced from the north, inter-digitate with deposits of the Sea Lion Fan.

274x184mm (300 x 300 DPI)



32  
33  
34  
35  
36  
37  
38  
39  
40  
41

Figure 13. Schematic depositional model for the Sea Lion Fan, and more generally a model for deep-lacustrine turbidite deposition. Lobe axis deposits are located in the more axial positions and are represented by thick successions of stacked, amalgamated, high-density turbidites that comprise structureless sandstone. The lobe axis deposits are focussed along sinuous corridors, controlled by partial confinement. The lobe fringe deposits comprise high-density turbidites that are typically thinner and less-amalgamated with greater preservation of fine grained, parallel to current ripple laminated bed tops along with the presence of more regular, thicker-bedded hemi-limnic mudstones. Hybrid event beds are observed in lobe fringe depositional locations, associated with the isolated occurrences of structureless sandstone. Lobe distal fringe deposits are dominated by low-density turbidites that largely comprise parallel-laminated to ripple laminated sandstones and preservation of pervasive hemi-limnic mudstones.

42  
43  
44  
45  
46  
47  
48  
49  
50  
51  
52  
53  
54  
55  
56  
57  
58  
59  
60

203x158mm (300 x 300 DPI)

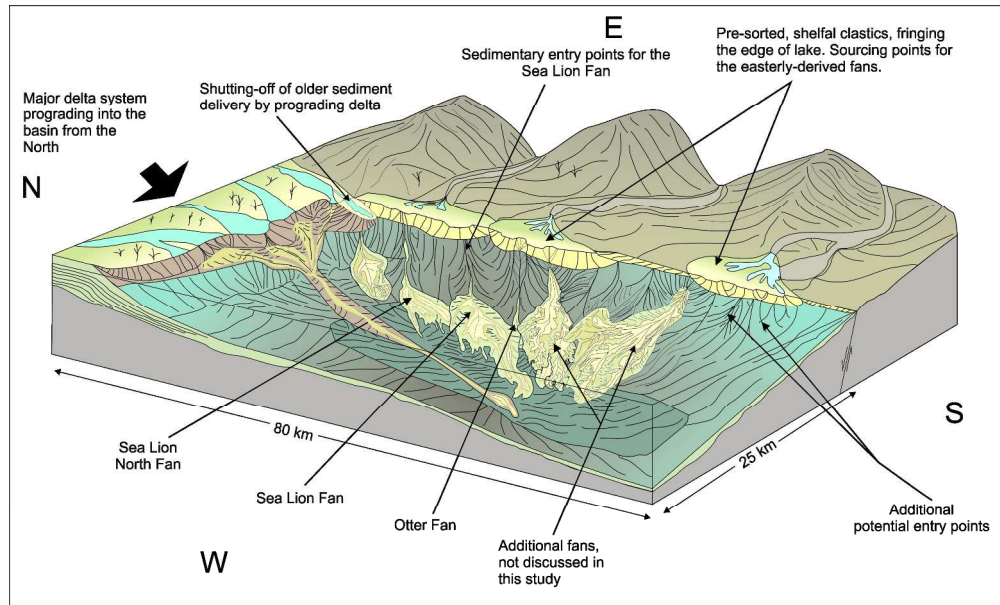


Figure 14. Schematic depositional environment for the NFB, during the Valanginian low-stand of the lake. A major axial delta prograded into the basin from the north, contemporaneously with the inclusion of the turbidite fans. These fans entered the basin from the eastern flank, forming sand-rich, slope apron features, draping the eastern basin slopes. Presence of detrital glauconite in these deposits suggests some element of pre-sorting in the shallow water environment, perhaps from a shelfal bar or fan delta. There is further evidence for Sea Lion-style fans, both geographically and stratigraphically throughout the NFB, indicating the potential for high sedimentation rates in the basin throughout the early Cretaceous.

288x173mm (300 x 300 DPI)

Facies Code	Facies Title	Facies Descriptions	Interpretation	Example
<i>frxls</i>	ripple cross laminated sandstone	Fine-to-medium grained, ripple cross laminated sandstone, with darker, sometimes carbonaceous/argillaceous silt-grade material, usually defining the ripple fore-sets. The thicknesses of this facies ranges from 2-10 cm, occasionally reaching 15 cm.	Current ripples formed through traction in a decelerating turbulent flow.	
<i>fss</i>	structureless sandstone	Fine-to-coarse grained, well-sorted, sub-angular, quartz-dominated sandstone. Occasional dark coloured lithic grains and poorly developed argillaceous banding towards the top of the units. The facies comprises structureless sandstones with loaded bases, into underlying mudstones. Units of <i>fss</i> are found in stacked packages, up to 15 m in thickness, comprising up to 10 different amalgamated beds.	Rapid suspension fall-out from high density turbidite currents (Lowe 1982), with enhanced sorting controlled by extensive run-out distances.	
<i>fgss</i>	graded structured sandstone	Medium-to-coarse grained, moderate-to-well sorted, sub-angular to sub-rounded sandstone displaying a coarse-grained base, normally grading to fine grained sandstone in the upper 2-3 cm of the bed. This facies typically comprises massive bedding and parallel laminations, which are particularly present in the upper portion of the bed. The top 2-3 cm contain elevated concentrations of clay-grade material.	Deposition in the tractional zone beneath a dilute turbulent flow (Allen, 1984)	
<i>fplm</i>	parallel laminated mudstone	Dark grey to black coloured, homogeneous mud-to-silt grade, parallel laminated siliciclastic mudstones. The laminations are depicted by subtle variations in colour and grain size. This facies contains 3-10 cm wide, round siderite nodules that are scattered throughout.	Hemi-limnic suspension fall-out in the water column ("background sedimentation").	
<i>fmcs</i>	mudstone-clast rich sandstone	Fine-to-medium grained, well sorted, sub-angular, structureless sandstone that is mud-clast rich. This facies shares similar qualities to <i>fss</i> , with the addition of mud-clasts. Mud-clasts are elongated and range from 2 cm to 10 cm long, are sub-angular and are usually composed of mudstone or siltstone. They commonly display lithic grain armouring, indicating partial lithification prior to rip-up, entrainment and deposition.	Rapid suspension fall-out from high density turbidite currents (Lowe, 1982), with angular, armoured clasts indicating up-dip erosion (Haughton et al., 2003).	
<i>fism</i>	inter-bedded sandstone and mudstone	Inter-bedded sandstones and mudstones. Sandstones are characterised as: very fine grained, ranging to medium grained, well sorted, sub-angular to sub rounded, structureless, occasionally parallel laminated and ripple cross bedded. Mudstones tend to be <1 cm-thick, homogenous and parallel laminated. Common examples of water escape structures and loading. Bioturbation is rare.	Post-depositional "re-working", slumping and churning through bottom-water processes and rare bioturbation.	

Table 1). - Description and core photographs of sedimentary facies from the Sea Lion Fan

286x195mm (300 x 300 DPI)

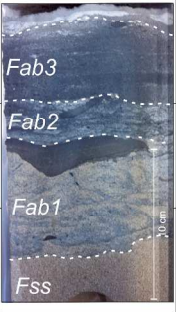
Facies Code	Facies Title	Facies Descriptions	Interpretation	Example
<i>fpls</i>	parallel laminated sandstone	Very fine-to-medium grained, well sorted, sub-angular, parallel laminated, normally graded sandstone. The parallel laminations are sometimes highlighted by clay-to-silt grade material in the matrix.	Fractional laminations formed by a waning flow (Allen, 1984).	
<i>fesm</i>	contorted (deformed) sandstone and mudstone	A chaotic assortment of mudstone and fine-to-coarse grained sandstone. Structuring includes: parallel laminations, dish structures, loading, ripple cross laminations particularly in the coarser sediments, along with common sections of poorly sorted, argillaceous-rich breccias. These units lack distinct boundaries and show complex geometries with over and underlying beds.	Slumping and re-mobilisation of soft sediments	
<i>frms</i>	rafted mudstone clast-rich sandstone	Poorly sorted, fine-to-coarse grained, structureless, sub-angular, clast-rich sandstone. Clasts are composed of a mixture of rounded mud-clasts and sub-angular to sub-rounded lithic fragments. The mud-clasts tend to be suspended in the middle-to-upper portion of the bed and are fully-supported by the matrix.	Freezing of a high concentration flow, whilst in a laminar state (Mutti and Nilsen, 1981). High-density suspension of mud-clasts (Postma et al., 1988)	
<i>fab3</i>	argillaceous breccia type 3	Very fine grained, argillaceous-rich (approx. >25%), poorly-sorted sandstones and siltstones. This facies contains some examples of elongate, flattened mud-clasts and relative concentration of 1-5 mm wide carbonaceous material in the matrix. This facies displays poorly formed laminations along which some of the mud-clasts rest.	Suspension fall-out from a disrupted/perturbed water column. This could also be viewed as deposition through longitudinal fractionation of lighter components (Houghton, et al., 2009)	
<i>fab2</i>	argillaceous breccia type 2	Very fine grained, argillaceous-rich (approx. 15%), crudely laminated sandstone. There is a marked increase in argillaceous material within the matrix compared to that of in <i>fab1</i> . Commonly, this facies comprises 1-5 cm long, elongated and/or flattened mud-clasts along with poorly formed parallel laminations.	En masse deposition in a cohesive flow (Houghton et al., 2009). Crude parallel laminations may represent sheared sand patches (Fonnesu et al., 2017)	
<i>fab1</i>	argillaceous breccia type 1	Very fine-to-fine grained, ripple laminated, poorly sorted sandstones, which display elevated argillaceous content (approx. 10%) within the matrix. There are common, 1-10 cm wide mud-clasts fragments within the matrix. Dewatering evidenced by dish structures has disrupted primary structuring, forming a chaotic "banding" of clean sandstone and light-grey coloured, clay-rich sandstone.	Transitional flow with intermittent turbulence suppression by dispersed argillaceous material (Houghton et al., 2009).	

Table 1 cntd.) - Description and core photographs of sedimentary facies from the Sea Lion Fan

286x195mm (300 x 300 DPI)